04
2020

BILINGUAL PUBLISHING CO.
Pioneer of Global Academics Since 1984

Volume 3 | Issue 4 | October 2020 | ISSN 2630-5119 (Online)

Journal of Atmospheric Science Research

ISSN 2630-5119
04
9 772630 511201

Volume 3 Issue 4 • October 2020 • ISSN 2630-5119 (Online)

Journal of Atmospheric Science Research

BILINGUAL PUBLISHING CO.
Pioneer of Global Academics Since 1984

BILINGUAL PUBLISHING CO.
Pioneer of Global Academics Since 1984

Volume 3 | Issue 4 | October 2020 | Page 1-43
Journal of Atmospheric Science Research

Contents

ARTICLE

BILINGUAL PUBLISHING CO.
Pioneer of Global Academics Since 1984

Journal of Atmospheric Science Research
https://ojs.bilpublishing.com/index.php/jasr

ARTICLE

Air Pollution in Kolkata: Emerging Challenges and Dynamics

Joy Karmakar*

Department of Geography, Serampore College, Hooghly

ARTICLE INFO

Article history
Received: 27 July 2020
Accepted: 10 August 2020
Published Online: 30 September 2020

Keywords:
Air pollution
Regulatory measure
Metropolitan area
Spatial and temporal change

ABSTRACT

In 2016 WHO reported that Kolkata is the second most polluted city in India behind Delhi. Albeit the number of registered vehicles in Kolkata is much less compare to Delhi. Kolkata has encountered a decade long battle against change of old vehicles and fuel types. So, this paper made an attempt to explore the dynamics of air pollution in the city specially pre and post period of vehicle and fuel change in the city. The objectives of the paper include looking at spatiotemporal change of air pollution in the city. Besides, the paper additionally illuminates on the role of land use functions and pollution in the city. The analysis shows that after the implementation of regulatory measures air pollution in the city reduced to some extent but effects of the measure gradually diminished. It is found that land use function as well as dynamics of metropolitan area plays crucial role in the air pollution of the city.

1. Introduction

Indian cities are profoundly polluted spaces. Measures of air quality in Indian urban areas show hazardously elevated levels of toxins and synthetics present noticeable all around. Concentrations of particulate matter are multiple times the levels in U.S. cities [1] and carbon monoxide, nitrogen oxides and benzene frequently far surpass the safety limits suggested by the World Health Organization (WHO). While there are several sources of this pollution, including industries in urban area, household fuel choices and the indiscriminate burning of leaves and other waste by municipal workers, vehicular pollution has come to be perceived as a main contributor [2]. World health organization identified six "classic" air pollutants generated from vehicular sources. These are lead, suspended particulate matter① (SPM), ozone, carbon dioxide, sulfur dioxide and Nitrogen dioxide. There are two significant fountains of vehicular contamination: First, the financial boom after 1990s joined with an insufficiency of public transport has prompted fast development in the sales of motorized vehicles. Second, most Indian cities are serviced by an ageing fleet of public and commercial vehicles, whose poor emissions attributes are aggravated by utilization of poor quality or debased fuel. An ongoing report by the Central Pollution Control Board in India expresses that 60 percent of vehicular pollution is inferable from vehicles that are more than 10 years of age and these form under 30 percent of the total populace of engine vehicles. Kolkata as one of the megacity in India also encounters poor air quality.

① The WHO places special emphasis on suspended particles smaller than 10 microns (μm) in diameter (PM10), also called inhalable particulate matter, and those smaller than 2.5 μm (PM2.5), called fine or respirable particulate matter

**Corresponding Author:*
Joy Karmakar,
Department of Geography, Serampore College, Hooghly;
Email: joykarmakar49@gmail.com

 DOI: https://doi.org/10.30564/jasr.v3i4.2231

In August 2003, based on Central Pollution Control Board (CPCB) data, the Supreme Court noted that the Respirable Particulate Matter (RSPM) levels in various Indian cities including Kolkata are alarming and directed the CPCB to work with local regulatory bodies to develop action plans to improve air quality. An investigation was completed with help from the Asian Development Bank (ADB) to survey the source of respiratory particulate matter in Kolkata in 2003. This investigation has anticipated that the respirable particulate outflows from vehicles, street dust, other area sources and industry will develop from an expected 75,140 to 136,796 tons for each year in 2014 if critical endeavors are not made to decrease emanations. It is likewise discovered that the most noteworthy outflows of suspended particulate matter (SPM) and PM_{10} have been seen at Kolkata. This could be because of the increased number of vehicles enrolled.

After years of legal and political bottlenecks, the Calcutta High Court also passed a judgment on July 18, 2008, ushering in a new regulatory regime for the city's transport system. All vehicles 15 years or more seasoned were restricted from the avenues and all auto-rickshaws were required to have 4-stroke motors that run uniquely on LPG. Following wide-spread viciousness in the city of Kolkata in January 2009 and requests from the state government, the court allowed a six-month augmentation until July 1, 2009. After several appeals and disagreements making a course for execution and when it occurred, was rushed as opposed to arranged. The city moved to LPG instead of compressed natural gas (CNG) which was known to have superior ignition properties and incite less damage to motor engines[3]. Therefore, maintaining good air quality in urban areas are not so linear rather a complex one. For instance, the imposition of fuel and vehicle emission standard can rise capital and operating expenses for transport operators. This may lead to the service unaffordable by poor users. So, transport policies have to be designed taking into considerations of environmental implications and public and private affordability. With this background the paper made an attempt to investigate whether the level of air pollution in Kolkata really reduced or remain as it was earlier even after change of fuel and engine of car. It is believed that several different dimensions in land use planning can also influence urban air quality. These dimensions of land use planning are inclusive of density, structure, diversity etc. [4,5]. Scholars showed that positive correlation exists between urban built up area and level air pollution. Thermal variations in urban area are also the results of different land use and land cover classes [6,7]. In this paper I examined the differences of air quality between the various measuring stations spanned across the city and air quality in different land use zones of the city. Moreover, the paper also analyzes the policies of late introduced to deal with the situation.

The following section provides the data, methodology and details of the site. Thereafter, air quality of the city is analyzed across spatial and temporal scale along with influence of land use function in the city. Then various policies introduced off late related to curbing air pollution are examined and in the last section concludes with some recommendations.

2. Data Base and Methodology

The Kolkata Municipal Corporation (KMC) covers an area of 187.3 km^2 and comprises of 141 wards extended to 15 boroughs. As per Census of India (2011), population of KMC in 2011 is 4,496,694. Density of the population in the city is 24,252 per sq. km. The city is situated along the banks of the Hooghly River. Temperature of the city ranges from 10^0C to 40^0C.

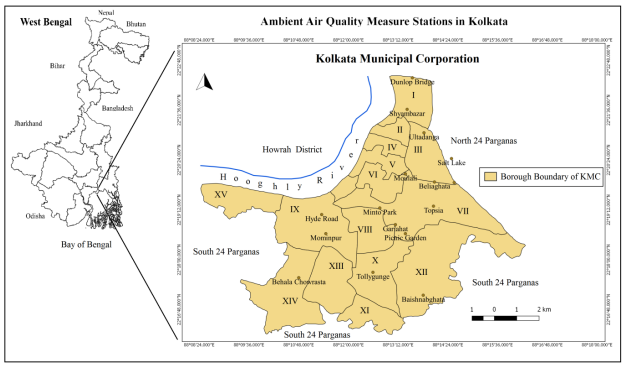

Figure 1. Kolkata Municipal Corporation (KMC) featuring Air Quality Monitoring Stations

It is a state capital and the only million plus city in the state of West Bengal. Air quality monitoring stations in the city are spread across the north, south, east and west part of the city. It is worthwhile to note here that to regulate pollution in the city in 2008 Calcutta High Court passed an ordered to change the vehicles engine and fuel.

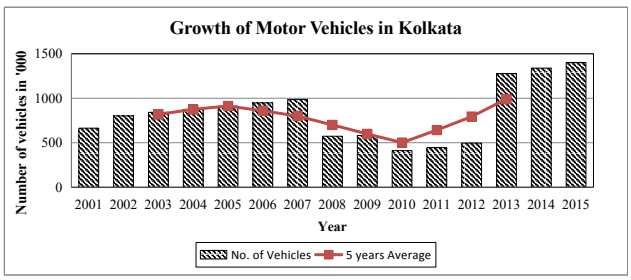

Figure 2. Growth of Motor Vehicles in Kolkata

Registered vehicles in the city sharply declined after the court order as evident in Figure 2; however number of cars

DOI: https://doi.org/10.30564/jasr.v3i4.2231

registered afterwards almost double. Though, more than fifty percent people used public transport as a mode for mobility in the city. In other words, car and two wheelers used only 10 percent of the people in the city [8]. Studies also show the positive relationship between increasing traffic volume and increasing pollution levels. A rough estimate indicate that per 1000 increase in traffic volume lead to an increase in NO_x level by 12.5 microgram per cubic meter, 150 microgram per cubic meter of SPM and 15.4 microgram per cubic meter of Hydro-carbon. In fact earlier studies in Kolkata showed that the highest polluting group is taxis of which 50 percent violates emission norms. Truck and private cars occupy second and third place with 39.2 percent violations and 32.6 percent violations respectively [9]. Therefore, growing numbers of vehicles in the recent years in city is a major concerned and argued one of the main contributors of the air pollution in the city.

The ambient air quality monitoring network includes estimation of various air toxins at various vital areas in the city. The West Bengal Pollution Control Board (WBPCB), under the direction of National Air Monitoring Program (NAMP), routinely screens ambient air quality of KMC. During the year 2017-2018, the board checked air quality in the district of Kolkata at 17 stations. Pollutants enter the cities as gases, particles, or as vaporizers, by dissipation of fluids or by co‐evaporation of dissolved solvents from water and by wind erosion. Significant air toxins in Indian cities are Sulfur dioxide (SO_2), suspended particulate matter, and nitrogen dioxide (NO_2). It is worthwhile to mention that in West Bengal only 4 stations measure the 12 parameters notified under National Ambient Air Quality Standard and rest of the stations (62 stations extend all over West Bengal) measure only three parameters i.e. SO_2, NO_2 and PM_{10}. For the purpose of this study 17 stations of KMC have been taken for analysis and all these station record above mentioned three standard parameters of air quality①. Moreover air quality data of 2008-09 is also taken for the analysis to understand temporal change in air quality of the city.

Based on the three parameters Air quality index (AQI) developed by Swamee and Tyagi [10] in 1999 has been used. AQI is determined by the following equation.

$$I= (\sum^{n}_{i=1}(AQI_i)^{p})^{1/p} \quad (1)$$

Where, I is the aggregate AQI

AQI_i=the sub-index for i^{th} pollutant, and p = a constant i.e. 2.5 as per Swamee and Tyagi.

① The checking of contaminations in these stations was completed for 24 h (four-hourly sampling for gaseous pollutants and eight-hourly sampling for particulate matter) with a recurrence of two times every week to have 104 perceptions in a year.

The sub index for i^{th} pollutant are measured through following equation

$$AQI_i = \sum_{i=1}^{N}\left((Si/q)^{m}\right) \quad (2)$$

Where, Si = sub-index, q = constant and m = constant

Since each of the constant varies with the pollutant following table is showing the details of the constant value

Table 1. Sub-index Constants

Pollutants	Units	q	m
Nitrogen dioxide	µg/L	3.75	0.94
Sulphur dioxide	µg/L	2.62	0.81
Suspended particulate matter 10	µg/L	1.00	0.87

Source: Swamee and Tyagi, 1999.

After the formulation of Air Quality Index (AQI) 17 stations have been categorized to test two hypotheses. The first hypothesis is that there is no difference of level of air pollution in the center and outer part of the city. The second hypothesis is that there is no difference of pollution among different land use of the city. To test the first hypothesis Mann-Whitney U② tests is used. The Null Hypothesis is that there is no difference of level air pollution between stations located at the centre and peripheries of the city. Following is the formula of U statistics [11].

$$\text{U test statistic} = \sum r - (n_r * (n_r+1)/2 \quad (3)$$

Moreover, to test second hypothesis Kruskal-Wallis H statistics has been applied. The null hypothesis is that there is no difference of air pollution level in the residential, commercial, industrial and mixed use area of the KMC. Following is the formula of H statistics

$$\text{H test statistic} = \frac{12}{N(N+1)}\left[\sum R^2/n\right] - 3(N+1) \quad (4)$$

Where, N= total sample size, n= the sample size of a particular sample, R = sum of the ranks of the particular sample, R^2 = square of the R, $\sum R^2/n$ = for each of the k samples quantity R^2/n is calculated then sum of these k quantities is taken.

② To begin with, the observations are arranged in ascending order in regard of the variable and their positions (R) are assigned (smallest value assigned rank 1, second rank 2 and so on). The subsequent advance includes arranging the observations' rank scores as per the sample or group to which they belong. The rank scores are added for these two groups of observations and the smaller total is assigned ∑r. The estimation of this amount is inserted into the equation for the test statistic along with nr - the number of observations in the group that provides ∑r.

 DOI: https://doi.org/10.30564/jasr.v3i4.2231

The following table 2 shows the air quality monitoring stations under different categories of location and its associated land use functions in the city. Only four major land use functions have incorporated for the analysis. These are residential, industrial, and commercial and mixed use. It is worthwhile to note that each of the land use function have taken into consideration for analysis due to its potential to produce air pollution.

Table 2. Classifications of the Air Quality Monitoring Stations

Stations	Location	Land use	Stations	Location	Land use
Dunlop Bridge	Edge	Industrial	Baishnabghata	Edge	Residential
Picnic Garden	Central	Residential	Ultadanga	Edge	Industrial
Tollygunge	Central	Mixed	Mominpur	Central	Industrial
Hyde Road	Edge	Industrial	Moulali	Central	commercial
Behala Chowrasta	Edge	Residential	Shyambazar	Central	commercial
Beliaghata	Central	Mixed	Gariahat	Central	commercial
Salt Lake	Edge	Residential	Minto Park	Central	commercial
Topsia	Central	Mixed	Paribesh Bhavan	Edge	Residential

Source: Compiled by the author.

Locational categories are done precisely on the basis of their relative location (from centre) in the city while land use category of the location are done based on recent classification of the land use of the city [12]. Though it is always difficult to draw sharp lines of demarcation between various lands uses in the city noted even perspective plan prepared by KMDA [13].

3. A Spatial and Temporal Comparison of Air Pollution in the City

Kolkata is the third most polluted city as far as nitrogen oxide (NOx) levels and twelfth most contaminated city as far as PM_{10} levels as per the announcement given by Ministry of Environment and Forests to Lok Sabha in August 2010 [14]. However, air quality varies across areas in Kolkata just as it vacillates every year. The pollution concentration in Kolkata is an element of blending profundity, wind speed, and physical size of the city. The occasional variety is likewise impacting the concentration of pollution in the city. The concentration of particulate toxins during winter is moderately higher than the remainder of the year in Kolkata (India). It is a result of the longer residence time of particulates in the environment, during winter because of low breezes and low blending height. In fact, air quality in Kolkata and it surrounding districts remains poor in winter and improves slightly in summer. Kolkata is noted for high use of diesel, to the extent that it has earned the designation of being the "diesel capital of the country". Harmful emissions from diesel vehicles are a huge concern in the city. Diesel vehicles contribute most extreme to the particulates, nitrogen oxides; harmful hydrocarbons that are the major concern for the quality of air in Kolkata. As indicated by CPCB assessment 55 percent of vehicles in Kolkata are diesel-driven [15]. While every commercial vehicle including the taxi runs on diesel, a significant number of these were also old. At present, the share of diesel vehicles is increasing. The World Bank examination of 2004 has surveyed that diesel ignition in the city can contribute essentially to the total $PM_{2.5}$ levels. During winter the proportion can go as high as 62 percent of the PM2.5 loads [16]. The following maps shows change of NO_2, SO_2 and PM_{10} between the year 2009 and 2018 across the different stations in the city.

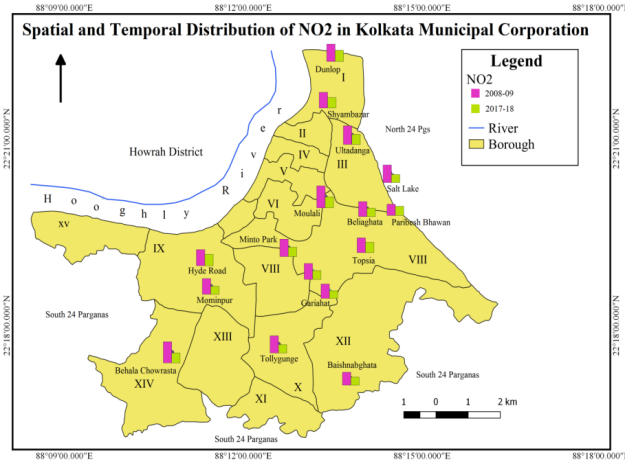

Figure 3.

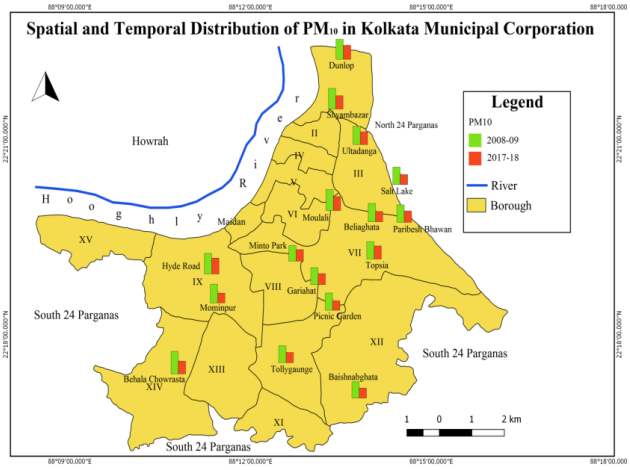

Figure 4.

DOI: https://doi.org/10.30564/jasr.v3i4.2231

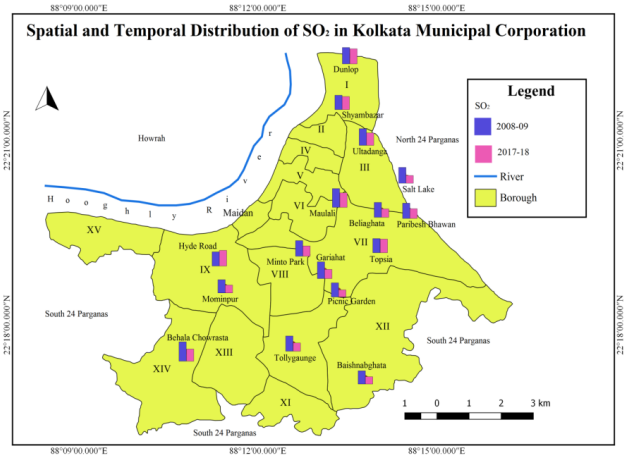

Figure 5.

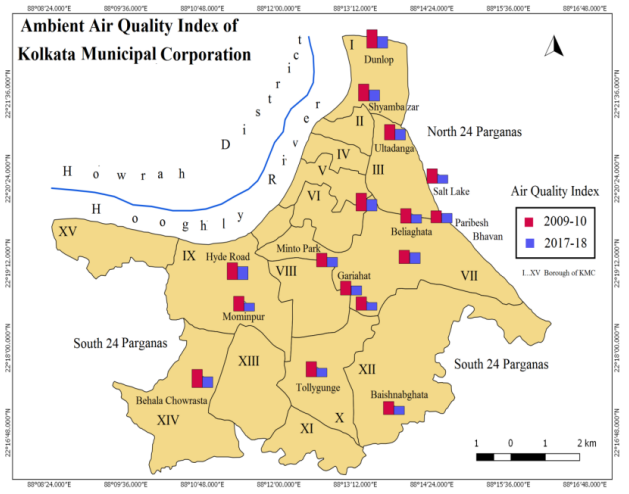

Figure 6.

Spatial distribution of the pollutants (Figure 3, 4 and 5) in KMC is also shows that level of air quality varies across the 17 stations. NO_2 was higher in 2008-09 in stations like Moulali, Ultadanga, Behala Chowrasta, while in 2017-18 the amount of NO_2 emission has reduced almost 50 percent across the 17 stations. Likewise PM_{10} emission in 2008-09 was higher at stations like Dunlop Bridge, Hyde Road, Behala Chowrasta, Moulali and Shyambazar. Emission of these stations reduced almost half after a decade. Similarly SO_2 emission was remain higher in stations like Dunlop Bridge, Moulali, Ultadanga, Salt Lake and Gariahat in 2008-09. In 2017-18 emission of SO_2 reduced in 10 stations but it remain higher in stations like Dunlop Bridge, Hyde Road, Moulali and Topsia. This improvement of air quality in the city is due to the various reasons inclusive of actions on vehicles and its fuel, regulation and shifting of industries. Moreover, it is found that there is an overall improvement of air quality. The above figure 6 shows the spatial and temporal change of air quality across 16 stations. Air quality index improves in all the stations ranging from 3 percent to 7 percent fall or improve across the 16 stations from 2008-09 to 2017-18 depicted in the figure 7.

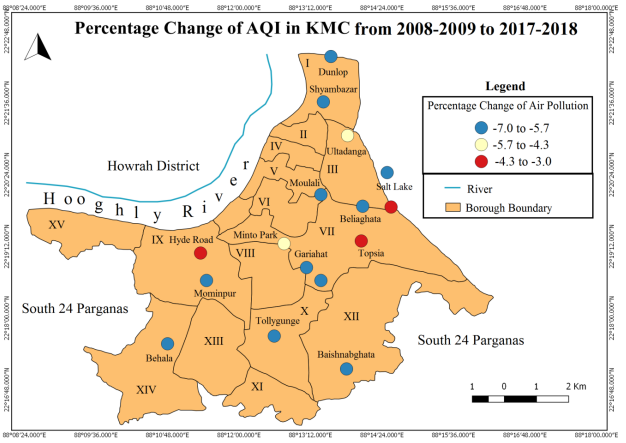

Figure 7.

It is evident from the above figure 7 that air quality index improves in all stations however; the improvement varies across the 16 stations. Out of 16 stations only four stations improve moderately inclusive of Hyde Road, Ultadanga, Topsia, and Paribesh Bhavan. 10 stations air quality index improves relatively higher and these stations include Behala Chowrasta, Tollygunge, Mominpur, Baishnabaghata, Gariahat, Minto Park, Beliaghata, Shyambazar, and Dunlop Bridge. As noted earlier that one of the significant factors that lies behind the improvement of the ambient air quality is the reduction of vehicular emission①. Nonetheless, registered vehicles increase twice in the city. So, change of vehicle engine and fuel became effective in the city.

Due to change of fuel and old vehicles, the air quality of the city improved gradually however, this improvement is not uniform across the monitoring stations as pointed out in figure 7. So to explore this arguement, "U" statistics is used and the Null Hypothesis is that there is no difference of air quality between monitering stations located at the centre and edge of the city.

Table 3. U Statistics Testing Air Quality between Centre and Periphery Stations

Year	Calculated Value
2007	38*
2017	30*

Source: Calculated by author, 2020, *tabulated value 53 at 5% level of significance and 57 at 2 % level of significance.

① Shifting of industries from inner city to city periphery started in Kolkata since 1996 through apex court order. Mainly tanneries of Kolkata were shifted to Bantala area. It was done reluctantly.

DOI: https://doi.org/10.30564/jasr.v3i4.2231

From the table 3 it is evident that null hypotheses is not rejected which means that level of air quality does not varies across the centre and peripheral monitoring stations of the city. No significant variation of the air quality in the centre and edge stations indicates that peripheral areas of the city is also growing fast[17]①. This growth is often the results of family migration from adjacent areas or from other areas within the state[18]. Some of the edge areas are recently incorporated into KMC. This areas are often encounters lack of public transport. The multi story housing developed in these area are with large parking facilities at the ground floor.

4. Land Use and Air Pollution in the City

As a rule, compact (that is mixed-use and high-density) urban structure is contrarily corresponded with auto reliance and positively correlated with the utilization of public transit and strolling, and along these lines the alleviation of air contamination [19]. The connection between urban structure and air contamination has been evaluated empirically using a variety of methodologies, especially in relation to developed countries [20]. McCarty and Kaza (2015) explored the relationship between several urban landscape metrics and AQI in the U.S., associating sprawling and fragmentary urban spatial structure with lower air quality [21]. Stone (2008) evaluated the relationship between urban structure and O_3 levels in 45 large U.S. metropolitan areas, finding that excessive O_3 levels were bound to happen in decentralized metropolitan areas than in spatially compact metropolitan regions [22]. Similar conclusions were drawn by Schweitzer and Zhou (2010) in their investigation of neighborhood-level O_3 concentration in 80 U.S. metropolitan districts [23]. Mansfield et al. (2015), and Hixson et al. (2010), have both researched the effects of different development scenarios on $PM_{2.5}$ fixations, coming to the same conclusion that compact development diminished these concentrations, while sprawling development increased them [24]. An investigation by Bechle et al. (2011) measured the impacts of urban structure on NO_2 concentrations for 83 cities globally, finding a negative relationship between urban contiguity and NO_2 focuses, and no statistically significant correlation between compactness and NO_2 concentrations [25]. Conversely, Borrego et al. (2006) inferred that compact urban morphology with mixed land uses assisted with bringing down NO_2 concentrations [26,27].

① Rapid growth of Kolkata's periphery is a recent phenomenon primarily after 1990s. it is worthwhile to mention here that Beery and Kasarda (1977) in their paper noted that around the periphery of the city were to be found poorest residents of the city, the schedule caste and refuges from East Bengal. With the passage of time these areas changed

Basic structure of the Kolkata's land use was laid out during the imperial rule and major elements of the city land use were associated with port function, the functions of central business and administrative region, the whole sale market area and European and native residential area. In the post-independence period the city has grown impulsively in south primarily and later in east and south east direction.

It is argued that Kolkata's 'compact city' structure is a bit of leeway: Very high level of strolling, cycling and public vehicle trips are an impression of the manner in which the city is planned. Dense and closely built structures diminish travel separations and make the city progressively walkable. It is hence not an unexpected that 60 percent of the total trips produced in the Kolkata Metropolitan Area have a normal separation of less than 3-4 km. This makes strolling, cycling, para-travel and public vehicle very alluring and possible [28]. In fact, the Census 2011 for Kolkata revealed that astounding 89 per cent people of the city walk and use public transport. More than one-fourth of the working population is commute to work on foot; nearly one-third work from home. Nearly half of the working population commutes by bus, bicycle and train. The rest commute by private mode and other modes. Though, the new improvement in suburbia is turning out to be sprawl and gated with poor public transport network.

H statistics is used to see whether the land use function at all influence the level of air pollution in the city or not. A null hypothesis is that there is no difference of air pollution level in different land use zones of the city. So in other words we are assuming that different land use functions of the city emanates similar amount of pollutants in the air.

Table 4. H Statistics Testing Air Quality at Different Land Use Function

Year	Calculated Value
2007	84.16*
2017	49.02*

Source: Calculated by author, 2020, *tabulated value 7.81 at 5% level of significance and 11.35 at 1 % level of significance.

From the table 4 it is evident that the null hypothesis is rejected and alternative hypotheses are accepted. Therefore, it is clear that different land use function in the city produces different amount of pollutants as a result air quality varies across the monitoring station. For example Hyde road and Baishnabghata area located in the edge of KMC but air pollution level in Hyde road is more compare to Baishnabghata because the former area comes under industrial zone while latter falls in the residential area. Similarly Dunlop Bridge and paribesh bhavan both are located at the edge of the city but proliferate differ-

DOI: https://doi.org/10.30564/jasr.v3i4.2231

ent amount of air pollutant due to its land use functions. Dunlop Bridge is located close to a thermal power plant and many other small industries so air quality in that area remains poor. On the other hand air quality of paribesh bhavan is relatively better due to its location in the residential zone. Following table 5 shows the average AQI at different land use zones in the city.

Table 5. Mean AQI at Different Land Use Zones in Kolkata

Land use Functions	2017	2007
Residential	109.92	188.36
Industrial	134.94	200.30
Commercial	127.87	175.56
Mixed use	115.30	181.63

Source: Calculated by author, 2020.

An overview of the table 5 suggests that air quality was poor and very poor in industrial and residential as well as mixed use zones. It is improved over the decades. Maximum improved of air quality occurred in the residential zones in the city. One of the significant reasons behind the improvement is the use of electricity for household lighting and use of LPG as cooking fuel. As per census 2011, more than 96 percent household in the city use electricity for lighting and more than 64 percent people use liquefied petroleum gas (LPG). At the same time more than 24 percent household still use kerosene as cooking fuel, which is one of the prominent sources of air pollution at the household level.

5. Emerging Challenges and Policy Intervention

Despite the fact that the degree of air contamination diminished somewhat yet new difficulties are likewise experienced by the city. The International Institute for Applied Systems Analysis (IIASA) in Austria and the Council on Energy, Environment, and Water (CEEW) in New Delhi reported that Indian citizens are likely to breathe air with high concentrations of suspended particulate matter ($PM_{2.5}$) in 2030, even if India were to comply with its existing pollution control policies and regulations. In addition they noted that the Indo-Gangetic plain, covering parts of states such as Uttar Pradesh, Bihar, and West Bengal, has the highest population exposure to significant $PM_{2.5}$ concentrations [29]. Kolkata is one of the megacities situated in the Indo-Gangetic plain where people are exposed to high amount of $PM_{2.5}$. A 2016 World Health Organization (WHO) reports exhibited Kolkata was the second-most polluted Indian city, behind Delhi [30]. In 2019, a day after Diwali and Kali Puja, the Air Quality Index (AQI) near the Victoria Memorial was 282. The area is considered as lungs of the city. Likewise, the AQI at Rabindra sarabar and Eastern Command headquarters in the city recorded 345 and 333 respectively. It was shocked the environmentalist because AQI in these stations normally remain moderate.

Shockingly, Kolkata and its metropolitan areas including Howrah, Hooghly, North 24 Parganas, South 24 Parganas and Nadia have far less vehicles and ventures contrasted with the National Capital District (NCR), and blasting of sparklers during Diwali is likewise less. Notwithstanding, Kolkata remains among the most contaminated cities throughout the year in India consistently. The explanation for the city being so contaminated is the widespread utilization of kerosene blended diesel via auto rickshaw drivers in Kolkata Metropolitan Areas (KMAs) like Hooghly, Howrah, North 24 Parganas, South 24 Parganas and parts of Nadia. In Kolkata, the greater part of the auto rickshaws employ on LPG cylinders which is profoundly polluting since it contains about 60 percent butane and 40 percent propane [31]. Other than that, the most disturbing fact is about 50,000 illicit 'Vano' (automated vans) are running on kerosene oil, which is extremely risky and exceptionally polluting. In the suburbia, Vano are running on the streets, and nobody minds enough to hold onto these profoundly contaminating vehicles noted by the city environmentalist [32].

In January 2019, the government launched the National Clean Air Program (NCAP), a five-year activity intend to control air contamination, fabricate a pan-India air quality checking system, and improve resident awareness. The program centers around 102 contaminated Indian cities and intends to diminish $PM_{2.5}$ levels by 20-30 percent throughout the following five years. Under this program they have identified “non-attainment cities” and Kolkata is one of the top most non-attainment cities in their list. To attain clean air in city some of the following suggestion has been made.

A real time data needs to be generated through mobile application and the application permits a user to rapidly and effectively produce straightforward reports about particular industry and its type①. Moreover, non-attainment cities require broad planation drive at polluting hotspot areas inclusive of traffic intersections, industrial zones, pathways, dust prone areas. Specialized plants have to be

① West Bengal State Pollution Control board categorizes industry into five types inclusive of red, orange, green and white types. In red and orange category there are 74 and 19 industry listed respectively. While in case of green and white category there are 67 and 37 industry listed. Beyond these four categories there is an exempted category of industries. Red and orange category of industries cannot be set up in Kolkata Metropolitan Areas (KMA).

 DOI: https://doi.org/10.30564/jasr.v3i4.2231

planted not only to purify air but also to improve health. Pollution abatement policies have to be implemented such as stringent norms for fuel and vehicles, fleet modernization, electric vehicle policies, and use of clean fuels etc. Mechanical sweeping and watering on road has to be done to control the dust in the city. In addition, specific guidelines and protocols have to be made to monitor and manage indoor pollution in the city. To implement this State Action Plan for Air Pollution has to be formulated.

6. Conclusion

This paper made an endeavor to examine the elements of urban air quality in Kolkata. There were a few difficulties in the last decade to control vehicle discharge and keep environment clean in the city. A portion of the administrative measures have been executed exclusively in the KMC however at metropolitan level administrative estimates remains unimplemented. Despite the fact, that air contamination in the city diminished for time being because of administrative measure however, it indeed began to increment. The paper likewise noticed that air quality in the city fluctuates over the diverse land use zones rather than center and edge of the city.

Conflicts of Interest

The author declares no conflicts of interest.

Availability of Data

All the data are accessed from online and available in government website and can be provided if required

References

[1] Greenstone, M., Rema, H. Environmental regulations, air and water pollution and infant mortality in India, NBER Working Paper 17210, 2011.

[2] Ghose, M. R. Paul, Banerjee, K.S. Assessment of the impacts of vehicular emissions on urban air quality and its management in Indian context: the case of Kolkata (calcutta), Environmental Science & Policy, 2004, 7(4).

[3] Ghosh, P., Somanathan, R. Improving Urban Air Quality in India Lessons from the Kolkata Clean Air Regulations of 2009, Working paper, International Growth Centre, London, 2013.

[4] Tolley, G. Cohen, A. Air pollution and urban land use policy, Journal of Environmental Economics and Management, 1976, 2(4).

[5] Weng, Q., Yang, S. Urban air pollution pattern land use and thermal landscape: an examination of linkage using GIS, Environmental Monitoring and Assessment, 2006, 117: 463-489. https://doi.org/10.1007/s10661-006-0888-9

[6] Nichol, J. E. High resolution surface temperature patterns related to urban morphology in a tropical city: A satellite bases study, Journal of applied Meteorology, 1996, 35(1).

[7] Balling, R. C., Brazell, S. W. High resolution surface temperature patterns in a complex urban terrain, Photogrammetric Engineering and Remote sensing, 1988, 54(9).

[8] National Transport Development Policy Committee. India Transport Report, Moving India to 2032, Routledge, New Delhi, 2013.

[9] Kolkata Metropolitan Development Authority. Perspective plan of KMA: 2025, KMDA, Kolkata, 2005.

[10] Swamee, P.K., Tyagi, A. Formation of an Air Pollution Index, Journal of the Air & Waste Management Association, 1999, 49(1): 88-91. DOI: 10.1080/10473289.1999.10463776

[11] Matthews, J.A. Quantitative and Statistical approaches to Geography, Pergamon press, Oxford.

[12] Nath, B, Acharjee, S. Urban Municipal Growth and Landuse Change Monitoring Using High Resolution Satellite Imageries and Secondary Data, Studies in Surveying and Mapping Science, 2013, 1(3).

[13] Munshi, S.K. Calcutta: Land, Land use and land market, chapter in books (Ed) Calcutta's Urban future: Agonies from the past and prospects from the future, by Dasgupta, B, Bhattacharya, M. Basu, D. K. Chatterjee, M. and Banerjee, T. K. Government of West Bengal, 1991.

[14] Roy Chowdhury, A. Citizen's report: Air quality and mobility in Kolkata, Centre for Science and Environment, New Delhi, 2011.

[15] Roy Chowdhury, A. Citizen's report: Air quality and mobility in Kolkata, Centre for Science and Environment, New Delhi, 2011.

[16] Gwilliam, K. Kojima, M. and Johnson, T. (2004) Reducing Air Pollution from Urban Transport, the World Bank, Washington DC

[17] Berry, B. J.L., Kasarda, J.D. Contemporary urban ecology, Macmillan, New York, 1977.

[18] Shaw, A. Inner-city and outer-city neighbourhood in Kolkata: Their changing dynamics Post liberalization, Environment and Urbanization Asia, 2015, 6(2): 139-153

[19] Frank, L.D., Sallis, J.F., Conway, T.L. Chapman, J.E., Saelens, B.E. Bachman, W. Many pathways from land use to health: Associations between neighborhood walkability and active transportation, body mass index, and air quality. Journal of American Planning Association, 2006, 72: 75-87.

DOI: https://doi.org/10.30564/jasr.v3i4.2231

[20] Marquez, L., Smith, N. A framework for linking urban form and air quality, Environmental Modeling and Software, 1999, 14(6): 541-548. https://doi.org/10.1016/S1364-8152(99)00018-3

[21] McCarty, J., Kaza, N. Urban form and air quality in the United States. Landscape and Urban Planning, 2015, 139: 168-179.

[22] Stone, B., Jr. Urban sprawl and air quality in large US cities, Journal of Environment Management, 2008, 86(4): 688-698.

[23] Schweitzer, L., Zhou, J. Neighborhood air quality, respiratory health, and vulnerable populations in compact and sprawled regions, Journal of American Planning Association, 2010, 76: 363-371

[24] Mansfield, T.J., Rodriguez, D.A., Huegy, J., Gibson, J.M. The effects of urban form on ambient air pollution and public health risk: A case study in Raleigh, North Carolina. Risk Anal, 2015, 35: 901-918

[25] Bechle, M.J., Millet, D.B., Marshall, J.D. Effects of income and urban form on urban NO2: Global evidence from satellites, Environmental Science Technology, 2011, 45(11): 4914-4919

[26] Borrego, C., Martins, H. Tchepel, O. Salmim, L. Monteiro, A., Miranda, A.I. How urban structure can affect city sustainability from an air quality perspective. Environmental Modeling and Software, 2006, 21: 461-467

[27] Wang, S., Fang, C., Wang, Y. Spatiotemporal variations of energy-related CO2 emissions in China and its influencing factors: An empirical analysis based on provincial panel data. Renewable Sustainable Energy Reviews, 2016, 55: 505-515.

[28] Roy Chowdhury, A. Citizen's report: Air quality and mobility in Kolkata, Centre for Science and Environment, New Delhi, 2011.

[29] International Institute for Applied Systems Analysis and Council on Energy Environment and Water. Pathways to Achieve National Ambient Air Quality Standards (NAAQS) in India, IIASA and CEEW, New Delhi, 2019.

[30] WHO. Ambient Air Pollution: a global assessment of exposure and burden of disease, World Health Organization, Geneva, 2016.

[31] Nath, S. Why Despite Fewer Vehicles and Industries, Kolkata is Chasing Delhi on Pollution Charts, News 18, 2019. Retrieved from: https://www.news18.com/news/india/why-despite-fewer-vehicles-and-industries-kolkata-is-chasing-delhi-on-pollution-charts-2378547

 DOI: https://doi.org/10.30564/jasr.v3i4.2231

BILINGUAL PUBLISHING CO.
Pioneer of Global Academics Since 1984

Journal of Atmospheric Science Research
https://ojs.bilpublishing.com/index.php/jasr

ARTICLE

Long-term Climatic Changes in the Northeastern Baikal Region (Russia)

Tatiana L. Ananina[1,2*] **Alexander A. Ananin**[1,2]

1. Federal State Establishment "United Administration of Barguzinsky State Nature Biosphere Reserve and Zabaikalsky National Park", Russia
2. Institute of General and Experimental Biology SB RAS, Russia

ARTICLE INFO

Article history
Received: 3 August 2020
Accepted: 20 August 2020
Published Online: 30 September 2020

Keywords:
Temperature
Precipitation
Oceanite
Continentality
Hydro thermality
Phenological border
Baikal

ABSTRACT

Due to global climate change it is important to constantly monitor the current climate state, observed trends and timely detection of their changes. The change in the hydrothermal regime has to result into changes in natural ecosystems. The analysis of long-term changes of mean annual temperatures and annual precipitation in warm and cold seasons over 1955-2017 years was carried out using data of the Davsha meteorological station , 54, 35˚N., 109,5˚E. Significant warming in the Northern Baikal region has been observed since 1990 and continues to the present. The climate is subcontinental with cool and short summers, frosty and long winters. In the last decade, there has been a shift of the beginning some phenology seasons. This had an effect on the increase in the warm season of the year and the duration of the frost-free period (by 5 days from the long-term average date). Spring comes earlier - for 3 days, summer and the last frost - for 5 days, autumn comes later - for 2 days.

1. Introduction

Comparison of the series of average annual air temperatures in the northern, southern hemispheres and the globe shows their consistency: warming from the beginning of the 20th century to the 40th gave way to some cooling until the midle 70ty, after which the warming continues to the present [1].The problem of climate change and the biota response to it became one of the most discussed issues. The local climatic conditions vary with global and regional climate change [2,3]. So, monitoring of local climate change and its impact on ecosystems is of great importance [4,5]. The change in the hydrothermal regime has to result into changes in natural ecosystems. In the Dolomites of Italy, in habitats above the forest boundary, several cold-loving species of the genus *Carabus* have disappeared over the past three decades. Scientists attribute this fact to the reaction of species to climate warming [6,7].

Regular observations of the climate in the Barguzin State Nature Biosphere Reserve, (Northern Baikal) cover the period from the late thirties. The most complete data obtained from the second half of the 20th century since 1955 at the eight time meteorological Davsha station of the second category. Significant warming in the Northern Baikal region observed since 1990 and continues to the

**Corresponding Author:*
Tatiana L. Ananina,
Federal State Establishment "United Administration of Barguzinsky State Nature Biosphere Reserve and Zabaikalsky National Park", Russia;
Institute of General and Experimental Biology SB RAS, Russia;
Email: t.l.ananina@mail.ru

DOI: https://doi.org/10.30564/jasr.v3i4.2255

present [8]. Thus, a change in the temperature regime of the Northern Baikal region had a corrective effect on the level of abundance of epigeobiont species of the genus *Carabus*. In recent decades, in response to an increase in temperature, all species have observed a reaction in the form of a burst of abundance exceeding the long-term average values. Changes in the temperature regime of the northern Baikal region had a corrective effect on the abundance of epigeobiont species of the genus *Carabus*. In recent decades, in some species, in response to temperature increases, there was a surge in abundance exceeding the long-term average values [9]. Transformations of the seasonal timing of registration of phenological phases in the life cycles of individual bird species are real responses to long-term climatic changes [10,11].

This paper analyzes long-term series of the mean annual temperature, the amount of annual precipitation and their combinations in the Northeastern Baikal region for the period 1955-2017. Analysis of long-term dynamics hydro thermality indexes, frost-free period duration, thermal boundaries of phenological seasons, snow cover, first and last frost are presented.

According to the authors Ed. Stonevicius and others (2018) [12] the continentality index most accurately reflects its local climate changes in the Northern Hemisphere. These authors claim that a statistically significant increase in continentality has only been found in Northeast Siberia. Therefore, to characterize the long-term temperature series of the Northeastern Baikal region, along with other indicators, we used index continentality and index oceanite also. Monitoring of climatic parameters was carried out on the territory of the Barguzin State Nature Biosphere Reserve. It is located on the northeastern coast of Lake Baikal (Figure 1).

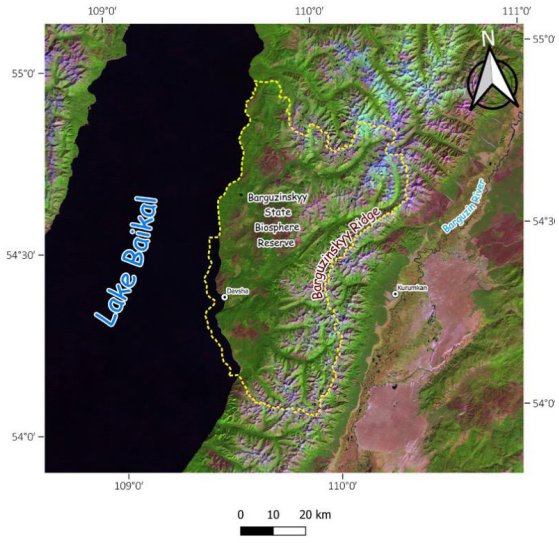

Figure 1. Location of the Barguzin State Natural Biosphere Reserve (North-Eastern coast of Lake Baikal)

The climatic conditions of the study area are determined, first of all, by its geographic location within the continent. Great influence on the climate by the proximity of Lake Baikal are lowering summer temperatures and the weakening winter frosts compared with adjacent territories [13]. The seasonal circulation of the atmosphere affects the formation of climatic conditions.

In winter, an area of high pressure is created near the surface of the earth, so the Asian (Siberian) anticyclone plays the main role (especially in January). In summer, on the contrary, the low-pressure baric field prevails; southern cyclones emerge from Mongolia into the Baikal region. Transitional autumn-spring seasons are characterized by the west-east transport of air masses. Also, in spring, cyclones from Central Asia and Kazakhstan periodically invade, in autumn meridional cold north winds break through. It is noted that autumn west-east movements are slower than spring ones [14].

2. Methods

The meteorological data were taken as a basis: average monthly and annual air temperatures, -monthly and annual atmospheric precipitation. Calculated indices applied: Average annual air temperature; Duration frost-free period (DFF, biological summer); Selyaninov hydrothermal coefficient (summer period) (HTC_S); Conrad continentality index (CCI); Kerner oceanity index (KOI). Phenological phenomena are indicative in the periodization of the annual cycle in nature. We analyzed the dates of the onset of the annual seasons.

DFF in a calendar year is the sum of days with an average daily temperature above 0 ºC.

HTI_S offered G.T. Selyaninov (1937) [15], it is used to determine dry and wet years. It takes volatility caused by the air temperature. HTC_S is equal to the ratio of the amount of precipitation for the period t>10 °C reduced by 10:

$$HTI_S = \Sigma P / \Sigma t * 10, \quad (1)$$

where ΣP = the amount of precipitation for the study period, Σt = the sum of the average daily air temperatures for the same period. This author proposes to consider the dry period during which the $HTI_S < 1.0$. In Russia, for the Eastern Siberia and the Far East, favorable conditions for moisture supply are created at $HTI_S = 1.3$ [15].

CCI formulas proposed by Conrad [16] and developed by Edvinas Stonevicius, 2018 and other researchers [12,17,18]. Climate continentality analyzed on the basis of the annual air temperature range [17,18]. In this research, continentality was evaluated using the equation:

$$CCI = 1.7 *(T_{max} - T_{min}) / Sin (\varphi + 10) - 14, \quad (2)$$

DOI: https://doi.org/10.30564/jasr.v3i4.2255

where T_{max} (°C) is the mean temperature of the warmest months of the year, T_{min} (°C) is the mean temperature of the coldest months of the year, and φ is the latitude.

A large annual range of air temperatures results in larger index values and consequently indicates a more continental climate. The smallest differences can be observed in the most oceanic climate conditions. The territories where index values range from (-20) to 20 can be described as hyper-oceanic, from 20 to 50 as oceanic, from 50 to 60 as sub-continental, from 60 to 80 as continental, and from 80 to 120 as hyper continental [11].

KOI represents the ratio of the mean monthly air temperature diference between October and April and the difference between mean monthly temperatures of the warmest and coldest months. Small or negative values indicate high continentality, whereas high index values indicate marine climate conditions [19]. The oceanity index (KOI) according to Kerner [20] was evaluated as follows:

$$KOI = 100 *(T_{oct} - T_{apr}) / (T_{max} - T_{min}), \quad (3)$$

where T_{oct} and T_{apr} (°C) are the mean monthly temperature in October and April, and T_{max} and T_{min} (°C) are the same as in CCI.

This index is based on the assumption that in marine climates, springs are colder than autumns, whereas in continental climates, springs demonstrates higher or similar temperatures as in autumn. The oceanity of the climate increases with index values. Small or negative values demonstrate continental climate conditions, while large values indicate a marine climate [21]. In order to visualise the spatial distribution of KOI, the following classes of index were used in this research: less or equal to (-10) - hypercontinental; from (-9) to 0 - continental; from 1 to 10 - subcontinental; from 11 to 20 - oceanic; and from 21 to 50 - hyper oceanic.

The timing of the onset of the seasons was selected according to the climatic criteria of the coastal zone of the Barguzinsky Reserve, proposed by K.P. Filonov (1978) [22]. Phenological seasons boundaries:

(1) Spring is the date of the final transition of maximum air temperatures above T (10°C);

(2) Summer is the date of stable transition of minimum air temperatures above T (5°C);

(3) Autumn is the date of transition of the minimum air temperatures below T (0°C);

(4) Winter is the date when permanent snow cover is established.

For graphical characteristics, the time series was divided into decades. The average indicators for six decades were compared: I - 1955-1964, II - 1965-1974, III - 1975-1984, IV - 1985-1994, V - 1995-2004, VI - 2005-2017 (12 days).

Standard statistical procedures Statistica 6.0 and Excel 2000 software package [23] to process the data set used. The contribution of trends to the long-term fluctuations of parameters was estimated by the Kendall rank correlation coefficient (R_τ, at $p < 0.05$) [24]. R_τ characterizes the percentage of variability of the long-term series.

3. Results and Discussion

Climate in the Northern Baikal region for the period 1955-2017 characterized by the following average annual indicators:

The mean annual temperature is (-3.4°C) at min (-6.1°C) and max (-1.2°C). The warmest months of the year are July (+12.9°C) and August (+13.5°C), the coldest months are January (-22.7°C) and February (-21.9°C).

The mean annual precipitation is 421 mm, with min 200 mm and max 660 mm. A greater amount of precipitation 251 mm (60%) falls in the warm season (May-September). Precipitation in the cold half of the year is 170mm (40%).

HTI_S is 2,5 with min 0,5 and max 4,7.

CCI is 56,9 with min 37,9 and max 70,4.

KOI is -10,9 with min -26,0 and max 0,5.

DFF is 117 days with min 95 days and max 140 days.

Dates of phenological events: Spring - May 24 (early May 8 and late June 14); Summer - July 4 (June 14 and July 27); Autumn - September 22 (September 7 and October 7), Winter - October 27 (October 5 and November 23). Term average last frost during the study period was June 14 (July 16 and May 19), the first frost - September 7 (August 10 and September 24. The snow cover finally established in October 27 (October 5 and November 23) and destroyed in May 6 (April 15 and May 25).

The frost-free period lasted on average 117 days (140 and 117 days).

Changes in the timing of the onset of the phenological seasons of the year are reflected in table 1.

Table 1. The characteristic phenology phenomena in Northeastern Baikal region in 1955-2017 (average for the decades)

Phenology phenomena, date of events	1955-1964	1965-1974	1975-1984	1985-1994	1995-2004	2005-2017	R_τ $p < 0.05$
Spring	24.05	28.05	24.05	24.05	19.05	21.05	0,2438
Summer	9.07	8.07	6.07	2.07	5.07	29.06	0,3104
Autumn	20.09	22.09	17.09	20.09	27.09	24.09	0,0338
Winter	23.10	24.10	25.10	31.10	30.10	27.10	0,2545
First frost	28.08	21.08	30.08	12.09	5.09	2.09	-0,3551
Last frost	26.06	15.06	17.06	11.06	11.06	9.06	0,4518
Snow setting	23.10	24.10	25.10	31.10	30.10	27.10	- 0,2545
Snow destruction	26.06	15.06	17.06	11.06	11.06	11.06	0,4863
Frost-free period (days)	110	107	115	123	122	122	0,5386

DOI: https://doi.org/10.30564/jasr.v3i4.2255

Thus, according to the analysis carried out, the climate of the Northern Baikal region can described as continental (subcontinental) with cool and short summers, frosty and long winters and above average precipitation. Precipitation is above average, most of it falls in summer. The cold period (with negative temperatures) averages 68%, and the warm period takes only one third of the calendar year. However, in the last three decades, there has been a shift of the beginning of the phenological seasons of summer and winter (first and last frosts). This had an effect on the increase in the warm season of the year, and, accordingly, on the increase in the duration of the frost-free period (by 5 days from the long-term average date). In the last decade, spring comes earlier - for 3 days, summer and the last frost - for 5 days, autumn comes later - for 2 days. The winter in the last decade comes exactly on the average long-term date, without changing, table 1.

The evolution of the mean annual temperature of the long-term series shown in Figure 2.

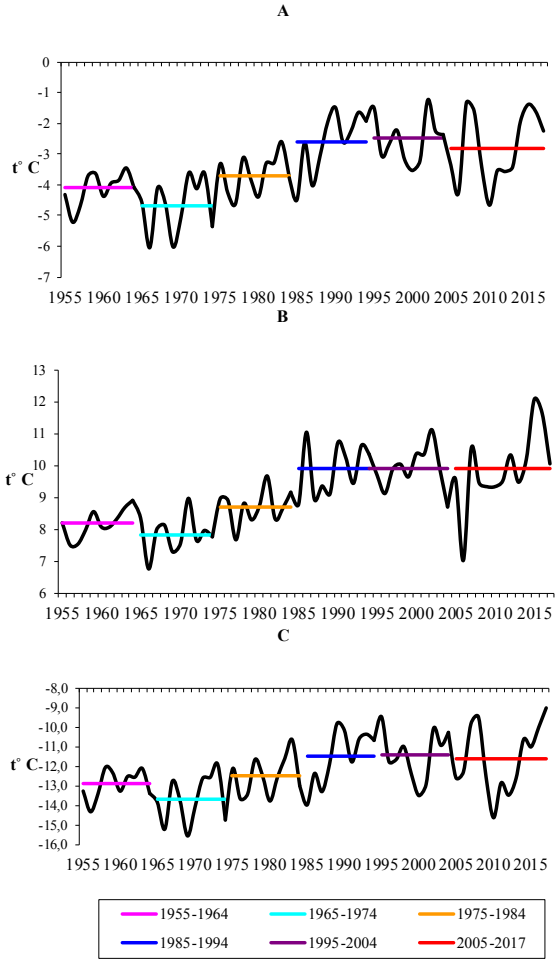

Figure 2. Dynamics of the average temperature for decades in the Northern Baikal region, A - average, B - warm season (May-September), C - cold season (October-April)

The contribution of the linear trend of the average annual temperature is R_τ = 0,4173, in the warm season - R_τ = 0,7060, in the cold season - R_τ = 0,5037. The amplitude of fluctuations in the mean annual air temperature is 6.5˚C. The linear trend of the mean annual air temperature is positive (correlation coefficient Tau = 0.421). The average long-term values in the previous periods of research: in 1955-1976. - (-4.1 ° C), 1955-1998 - (-3.7 ° C), 1955-2007. - (-3.1 ° C) [25], 2000-2017 - (-2.8 ° C), 1955-2015 - (-3.4 ° C). The average temperature for each of the 6 decades was higher in the fifth (-2.5˚C), maximum - (+ 0.4˚C) in 2004, lower - in the second decade (-4.7˚C), minimum - (-6.1˚C) in 1966, and (-6.0˚C) in 1969. A significant increase in air temperature was noted from the third decade (-3.7˚C), the maximum (-2.6˚C) in 1983. Since the fourth decade, the average annual temperature has remained constantly high (-2.6˚C), the maximum temperature for the last three decades was (-1.2˚C) in 2002 (Figure 2 A).

The evolution of the total annual precipitation and HTI_S shown in Figure 3

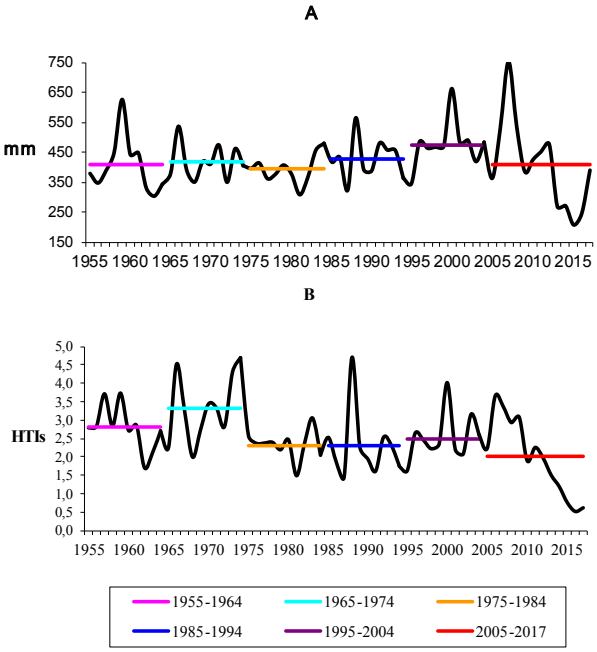

Figure 3. Dynamics of the total precipitation (A) and the Hydrothermal Index (B) for decades in the Northern Baikal region

The deviation of the amount of precipitation (R_τ = 0,0472) and, accordingly HTI_S (R_τ = 0,0892), in the dynamic series from the average long-term value was absolutely insignificant, except for the last decade R_τ = 0,3934 and R_τ = 0,4123. It is characteristic that in the sixth decade the largest amount of precipitation observed - 750.2 mm, in 2007 and the smallest - 205.9 mm, in 2015.

DOI: https://doi.org/10.30564/jasr.v3i4.2255

(Figure 3, A). A significant decrease in HTI_S noted since 2012, which contributed to a sharp increase in climate aridity (Figure 3, B) and fire hazard. This reflected in the frequency of forest fires in 2013, 2015, 2016 not only on the territory of the reserve, but throughout the entire Baikal region.

The dynamics of the indices of oceanicity and continentality shown in Figure 4.

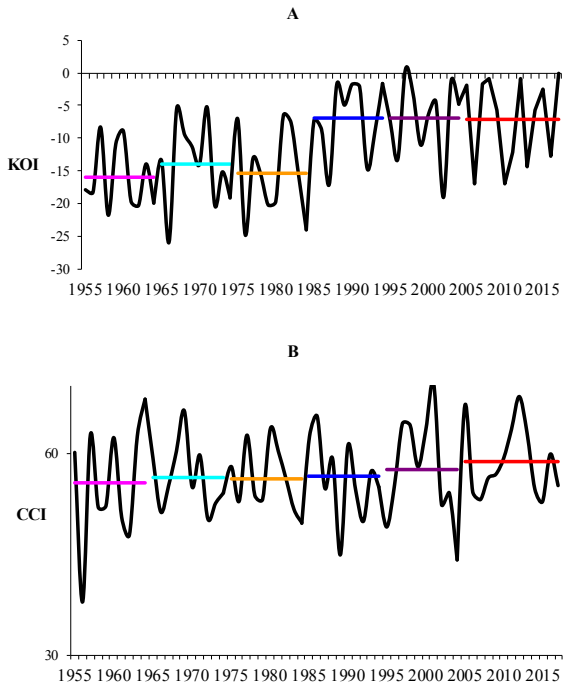

Figure 4. Dynamics of indexes KOI (A) and CCI (B) for decades

The dynamics of the CCI did not differ in large changes (R_τ = 0,1427) and the linear trend almost did not go beyond the stationary one (R^2 = 0204). On the contrary, the oceanic index (R_τ = 0,4959) and linear trend (R^2 = 0,2459) showed a significant decrease in the continentality of the climate over the past three decades since 1988 in the Northern Baikal region.

4. Conclusion

Over the past 62 years, significant climate change has been marked on Northern Baikal. The duration of the frost-free period increased due to the shift in the dates of the phenology borders beginning of spring, summer and autumn. With an increase in air temperature and with the same level of precipitation, the oceanity/continentality of the climate decreased significantly. A significant decrease in hydrothermal index noted since the beginning of the second millennium, which contributed to a sharp increase in climate aridity.

References

[1] Sokolov, L. V. Climate in the life of plants and animals. Saint Petersburg: Publishing house Tessa, 2010: 343.

[2] Nazimova, D. I., Tsaregorodtsev, V. G., Andreyeva, N. M. Forest vegetation zones of Southern Siberia and current climate change, Geography and Natural Resources, 2010, 31(2): 124-131.

[3] Luff, M. L. The carabidae (ground beetles) of Britain and Ireland. RES Handbook. Field Studies Council, Shrews-bury, 2007, 4(2): 247.

[4] Ananina, T.L., Ananin, A.A. Some results of monitoring the temperature regim in the altitude zone of the Barguzin Ridge (Northen Baikal region). Material of the International Conference (Birmingham, United Kingdom, 2019: 113-121.
DOI 10.34660/INF.2019.1.41068

[5] Pospelova, E. B., 1, Pospelov I. N., Orlov, M.V. Climate change in Eastern Taimyr over the last 80 years and the warming impact on biodiversity and ecosystem processes in its territory. Nature Conservation Research, 2017, 2(3): 215-221.
DOI: 10.24189/ncr.2017.040

[6] Ananin, A.A., Ananina, T.L., Darizhapov, E.A., Puzachenko, A.Yu., Fadeev, A.S. The influence of climate change on the biota of the Barguzin reserve. The influence of climate change on ecosystems. M .: Russian University, 2001, 2: 1-8.

[7] Brandmayer, P., Pizzalotto, R. Climate change and its impact on epigean and hypogean carabid beetles. Periodicum Biologorum, 2016, 118(3): 147-162.
DOI: 10.18054/pb.2016.118.3.4062

[8] Ananina, T.L., Ananin, A.A. Some results of temperature monitoring obtained using automatic meteorological instruments (Barguzinsky ridge). Natural complexes of the North-Eastern Baikal region. Proceedings of the Barguzinsky state natural biosphere reserve. FSE United Administration of Barguzinsky State Nature Biosphere Reserve and Zabaikalsky National Parc. Ulan-Ude: Publishing House of Buryat Scientific Center of the Siberian Branch of the Russian Academy of Sciences, 2019, 11: 183-189.
DOI: 10.31554/978-5-7925-9-11-2019-183-189

[9] Ananina, T.L. Results of longterm monitoring of the genus Carabus (Coleoptera: Carabidae) in the Barguzinsky range (Northern Baikal Region). Contemporary Problems of Ecology, 2020, 4: 491-503.
DOI: 10.15372/SEJ20200407

[10] Ananin, A. A. Formation and analysis of long-term series of bird population observations at key sites as a method of studying biodiversity. Contemporary

DOI: https://doi.org/10.30564/jasr.v3i4.2255

Problems of Ecology, 2020, 4: 479-490.
DOI: 10.15372/SEJ20200406

[11] Lehikoinen, A., Lindén, A., Karlsson, M., Andersson, A., Crewe, T. L., Dunn, E. H., Gregory, G., Karlsson, L., Kristiansen, V., Mackenzie, S., Newman, S., Røer, J. E., Sharpe, C., Sokolov, L. V., Steinholtz, Å., Stervander, M., Tirri, I. S., Tjørnløv, R. S. Phenology of the avian spring migratory passage in Europe and North America: Asymmetric advancement in time and in-crease in duration. Ecol. Indicat., 2019, 101: 985-991.

[12] Stonevicius Ed., Stankunavicius G., Rimkus, Eg. Continentality and Oceanity in the Mid and High Latitudes of the Northern Hemisphere and Their Links to Atmospheric Circulation. Advances in Meteorology, Article ID, 5746191, 2018: 12.
DOI: doi.org/10.1155/2018/5746191

[13] Ladokhin, N.P., Turcan, A. M. An outline of the local climate of the coastal zone of the Barguzinsky reserve. Proceedings of the Barguzinsky state reserve. Moscow, 1948, 1: 149-176.

[14] Ecological atlas of the Baikal basin. Irkutsk: Publishing house of the Institute of Geography. B. B. Sochava SO RAN, 2015, 145.

[15] Selyaninov, G.T. Methodology for agricultural characteristics of the climate. World Agroclimatic Directory. Leningrad-Moscow, 1937: 5-26.

[16] Conrad, V. Usual formulas of continentality and their limits of validity. Proceedings of the American Geophysical Union, 1946, 27(5): 663-664.

[17] Vil˘cek, J., ˘Skvarenina, J., Vido, J., Nalevankov´a, P., Kandr´ık, R., ˘Skvareninov´a, J. (2016). Minimal change of thermal continentality in Slovakia within the period 1961-2013. EarthSystem Dynamics, 1946, 7(3): 735-744.

[18] Gadiwala, S.M., Burke, F., T. Alam, M., Nawaz-ul-Huda, S., Azam, M. Oceanity and continentality climate indices in Pakistan. Malaysian Journal of Society and Space, 2013, 9(4): 57-66.

[19] Kerner, F. Thermoisodromen, Versuch einer kartographischen Darstellung des jahrlichen Ganges der Lufttemperatur (Wien). K. K. Geographische Gesellschaft, 1905, 6(3): 30.

[20] Andrade, C., Corte-Real, J. Assessment of the spatial distribution of continental-oceanic climate indices in the Iberian Peninsula. International Journal of Climatology, 2017, 37(1): 36-45.

[21] Hirschi, J. M., Sinha, B., Josey, S. A. Global warming and changes of continentality since 1948. Weather, 2007, 62(8): 215-221.

[22] Filonov, K.P. Seasonal development of nature in the Barguzinsky reserve. Natural complex of the Northeastern Baikal region. Proceedings of the Barguzinsky State Reserve. Ulan-Ude, 1978, 7: 47-67.

[23] Tyurin, Yu.N., Makarov, A.A. Statistical analysis of data on a computer/ed. V.E. Figurnova. M .: INFRA-M, 1978, 528.

[24] Pesenko, Yu.A. Principles and methods of quantitative analysis in faunistic research. M.: Nauka, 1982, 287.

[25] Ananina, T.L. Temperature factor in the life of the dominant species of ground beetles (Coleoptera, Carabidae) of the Barguzinsky ridge. Bulletin of the Samara Scientific Center of the Russian Academy of Sciences, 2010, 12(33), 1(5): 1260-1263.

 DOI: https://doi.org/10.30564/jasr.v3i4.2255

BILINGUAL PUBLISHING CO.
Pioneer of Global Academics Since 1984

Journal of Atmospheric Science Research
https://ojs.bilpublishing.com/index.php/jasr

ARTICLE

Assessing the Impacts of Climate Change on Crop Yields in Different Agro-climatic Zones of India

Naveen P Singh[1*] Bhawna Anand[1] S K Srivastava[1] K V Rao[2] S K Bal[2] M Prabhakar[2]

1. ICAR-National Institute of Agricultural Economics & Policy Research (NIAP), New Delhi, India
2. ICAR-Central Research Institute for Dryland Agriculture (CRIDA), Hyderabad, India

ARTICLE INFO

Article history
Received: 10 August 2020
Accepted: 27 August 2020
Published Online: 30 September 2020

Keywords:
Agro-climatic zones
Climate change
Crop yields
RCPs

ABSTRACT

The study attempts to estimate and predict climate impact on crop yields using future temperature projections under two climate emissions scenarios of RCP 4.5 and 8.5 for three different time periods (2030s, 2050s and 2080s) across Agro-climatic zones (ACZ) of India. During the period 1966-2011, a significant rise was observed in both the annual mean maximum and minimum temperature across ACZs. Rainfall recorded an annual decline in Himalayan Regions and Gangetic Plains and a rise in Coastal Regions, Plateau & Hills and Western Dry Region. Our results showed high heterogeneity in climate impact on *kharif* and *rabi* crop yields (with both negative and positive estimates) across ACZs. It was found that rainfall had a positive effect on most of crop yields, but was not sufficient enough to counterbalance the impact of temperature. Changes in crop yield were more pronounced for higher emission scenario of RCP 8.5. Thus, it was evident that the relative impacts of climate change and the associated vulnerability vary by ACZs, hence comprehensive crop and region-specific adaptation measures should be emphasized that helps in enhancing resilience of agricultural system in short to medium term.

1. Introduction

Climate change has emerged as the most potent global risk to the food security and agriculture-based livelihoods, impeding the pathway to sustainable development especially among the developing nations. The Intergovernmental Panel on Climate Change [1], states that greenhouse gas accumulation due to increased anthropogenic emissions has caused 1.0°C of global warming above the pre-industrial levels which is likely to reach 1.5°C between 2030 and 2052. Over the past years for different plausible scenarios, researches have well established the sensitivity of agriculture sector to the changing climatic conditions with concomitant implications for food security [2-5]. Agriculture production and productivity are directly influenced by changes in rainfalland temperature [6-9]. Temperature when exceed the critical physiological threshold adversely affects crop yield via increased heat stress on crops, water loss by evaporation and proliferation of weeds and pest [10]. Also greater erraticism in the distribution of rainfall resulting in drought or flood like situations induces crop failures through higher runoff, soil erosion and loss of nutrients. However, the magnitude of climate impact on agricultural production varies geographically based on agro-ecological zone, technological and socio-economic conditions

**Corresponding Author:*
Naveen P Singh,
ICAR-National Institute of Agricultural Economics & Policy Research (NIAP), New Delhi, India;
Email: naveenpsingh@gmail.com

DOI: https://doi.org/10.30564/jasr.v3i4.2269

[11]. Besides, location specific adaptation strategies and measures are adopted by the farmers premised on their economic and institutional capacity which are expected to shape the severity of climate impact. Such spatial disparities result in differential climate impact and projections for different crops, for instance, a 2ºC local warming in the mid-latitudes could increase wheat production by nearly 10 percent [12], whereas in low latitudes the same amount of warming may decrease yields by nearly the same amount. Though the impact of climate change on crop yields could be either positive ornegative; nevertheless, the past evidences generally postulate a negative effect of warming on crop production [13].

India, located close to the equator and in the tropics is disproportionately at a higher risk to the climatic aberrations. The country has diverse geographical and agro-climatic conditions which translate into differential regional impacts. Over the past decades acontinuous rising trend has been observed in both minimum and maximum temperature in the country [14,15,16,17]. Though for rainfall there are no clear long-term evidences of variations at the national level [18, 19] but regional analysis reveals a changing pattern of precipitation [20,21]. This poses enormous challenges for both food production and livelihoods of small-scale farmers' who are already hapless with limited financial resources and access to infrastructure to invest in appropriate adaptation measures [22,23].

In India, several studies have been undertaken to quantify the impact of climate change on crop yields. For instance, the reduction in major crop yields by 4.5 to 9 percent over the period 2010-2039 and by 25 percent in the long-run (2070-2099) without any long-run adaptations was predicted [24]. In another study projected that climate change will reduce wheat yield in the range of 6 to 23 percent by 2050 and 15 to 25 percent by 2080 [25]. Also rice yield will be lower by 15 percent and wheat yield by 22 percent towards end of the century [26]. By 2080- 2100 there is a probability of 10-40 percent crop loss in the country due to global warming [7]. Further, high losses in crop yield ranging from 30 to 40 percent have been projected by 2080, both with and without carbon fertilization [27]. By end of this century,the productivity of cereal crops like rice and wheat will be negatively impacted for 2-4°C increase in temperature and rise in the rate of precipitation[28]. Moreover, yields of wheat, soybean, mustard, groundnut and potato are expected to decline by 3-7percent for 1oC rise in temperature [29]. Most of the previous assessments have extrapolated climate impact on crop yields at a national and state level; however, there remains a considerable uncertainty over the likely climate impact for homologous environments. Hence, there is a dire need to get empirics related to the impact of climate change for major crops at agro-climatic zone level so that location specific R&D and dynamic, diversified and flexible interventions having local contexts can be suggested [30,31]. Thus, the present study examined the impact of climate variables on major *kharif* and *rabi* crop yields, across agro-climatic zones (ACZs) delineated by the erstwhile Planning Commission, Government of India [32] for the period 1966 to 2011. Further, the study projected the likely changes in crop yields for different time periods across the zones.

2. Agro-climatic Zones: Spread and Characteristics

Regional heterogeneity across the Indian geographical landscape significantly influence the growth and development of agriculture system, leading to existence of inter/intra-regional disparities in rural income and technology adoptions [33]. In the course of changing climatic conditions and depletion of natural resources base, sustainability of agriculture necessitates development of effective technologies and differentiated mechanisms that address region-specific farm-level issues. This requires constructing spatially disaggregated plans for homogeneous regions that bring synergy between the core components of technology for resource-use efficiency. The genesis of regionalization of national agriculture economy by Planning Commission goes back to 1989wherein the mainland of India was retrenched into 15 agro-climatic zones based on physical conditions, topography, soil, geological formation, rainfall pattern, cropping system, development of irrigation and mineral resources[34]. The regionalization exercise was undertaken with the prime objective of internalizing the resource development potentials and physical distinction across states/ regions in the country into the developmental policy and programme formulation and implementation [35]. Table 1, depicts the spatial characteristic of 14 agro-climatic zones (excluding the island region), wherein it was found that Southern Plateau & Hills (comprising parts of Andhra Pradesh, Karnataka and Tamil Nadu) and Eastern Plateau & Hills occupied the largest geographical area. Middle Gangetic Plains comprising Bihar and parts of Uttar Pradesh was the most populated, while Western Himalayan Region had the lowest population. Western Plateau & Hills had the largest net sown area of about 19.66 million hectares. This was followed by Southern Plateau & Hills and Central Plateau & Hills with a net sown area of approximately 18.08 and 16.78 million hectares, respectively. In case of food grain productivi-

 DOI: https://doi.org/10.30564/jasr.v3i4.2269

Table 1. Characteristics of Agro-climatic zones in India

Agro-climatic Zone	Climate	Annual Rainfall (mm) (1966-2011)	% Annual change Rainfall (1966-2011)	Annual MinT (°C) (1966-2011)	% Annual change MinT (1966-2011)	Annual MaxT (°C) (1966-2011)	% Annual change MaxT (1966-2011)	Area[$] ($Km^2$)	Population[P] (Persons)	net sown area (Mha)	food grains yield (Ton/ha)	States[@]
Western Himalayan Region	Cold Arid to Humid	1158.21	-0.3584***	14.18	0.2940***	26.27	0.0798***	331392 (10.08)	29492196 (2.44)	1.995	2.178	Himachal Pradesh (12,16.80), Jammu &Kashmir[w] (22, 67.06), Uttarakhand (13,16.14)
Eastern Himalayan Region	Per Humid to Humid	2463.50	-0.1972*	18.40	0.1552***	27.86	0.0591***	274942 (8.36)	54310943 (4.49)	4.916	1.828	Arunachal Pradesh (16, 30.46), Assam (27, 28.53), Manipur (9, 8.12), Meghalaya (7, 8.16), Mizoram (8, 7.67), Nagaland (11, 6.03), Sikkim (4, 2.58), Tripura (4, 3.81), West Bengal (3, 4.64)
Lower Gangetic Plains	Moist Sub Humid to Dry Sub Humid	1485.36	-0.0909	21.21	0.1167***	31.55	0.0259***	69730 (2.12)	79807245 (6.59)	4.204	2.659	West Bengal (15, 100)
Middle Gangetic Plains	Moist Sub Humid to Dry Sub Humid	1113.14	-0.1213	19.45	0.1277***	32.08	0.0460***	163793 (4.98)	169736896 (14.02)	9.704	1.590	Uttar Pradesh (23, 42.51), Bihar (38, 57.49)
Upper Gangetic Plains	Dry Sub-Humid to Semi-Arid	878.24	-0.4602***	18.87	0.1126***	32.28	0.0325***	141881 (4.32)	124493345 (10.28)	9.590	2.345	Uttar Pradesh (41, 100)
Trans Gangetic Plains	Extreme Arid to Dry Sub-Humid	672.73	-0.0730	18.26	0.1240***	31.90	0.0380***	147044 (4.47)	77045988 (6.36)	10.626	3.640	Chandigarh (1, 0.08), Delhi (9,1.01), Haryana (21, 30.07), Punjab (20, 34.25), Rajasthan (3, 34.60)
Eastern Plateau & Hills	Moist Sub-Humid to Dry Sub-Humid	1324.19	0.1026*	19.95	0.0729***	31.42	0.0140***	378178 (11.50)	91990522 (7.60)	10.461	1.560	Chhattisgarh (18, 35.75) Jharkhand (24, 21.08), Madhya Pradesh (5, 8.58), Maharashtra (3, 6.28), Odisha (17, 26.66), West Bengal (1, 1.66)
Central Plateau & Hills	Semi-Arid to Dry Sub-Humid	916.80	-0.2602***	19.13	0.1055***	32.00	0.0506***	334700 (10.18)	86527530 (7.15)	16.784	1.947	Madhya Pradesh (31, 58.58), Rajasthan (18, 32.63), Uttar Pradesh (7, 8.79)
Western Plateau &Hills	Semi-Arid	929.05	0.0567	19.95	0.0614***	32.91	0.0357***	332979 (10.13)	101767520 (8.40)	19.666	1.561	Madhya Pradesh (14, 23.94), Maharashtra (25, 76.06)
Southern Plateau & Hills	Semi-Arid	843.24	0.1237**	21.41	0.0747***	32.23	0.0479***	407014 (12.38)	132852963 (10.97)	18.082	2.720	Andhra Pradesh (15, 47.96), Karnataka (23, 37.10), Tamil Nadu (13, 14.94)
East Coast Plains & Hills	Semi-Arid to Dry Sub-Humid	1100.96	0.1334*	22.38	0.0750***	31.34	0.0454***	199900 (6.08)	94280839 (7.79)	7.205	2.076	Andhra Pradesh (8, 39.93), Odisha (13, 27.45) Puducherry (4, 0.25), Tamil Nadu (17, 32.37)
West Coast Plains & Ghats	Dry Sub-Humid to Per Humid	2417.93	0.0052	20.60	0.0545***	30.36	0.0376***	118634 (3.61)	75722655 (6.25)	4.299	1.366	Goa (2, 3.12), Karnataka (7, 34.39), Kerala (14, 32.75) Maharashtra (6, 25.90, Tamil Nadu (2, 3.84)
Gujarat Plains & Hills	Arid to Dry Sub-Humid	861.77	0.5244***	19.95	0.0369***	32.17	0.0203***	196846 (5.99)	61026648 (5.04)	7.931	2.036	Gujarat (26, 99.69), Dadra & Nagar Haveli (1, 0.25), Daman & Diu (2, 0.06)
Western Dry Region	Arid to Extremely Arid	427.54	0.1105	18.77	0.1155***	33.08	0.0545***	182157 (5.54)	31354633 (2.59)	9.727	1.962	Rajasthan (12, 100)

Source: Authors Compilation and Estimation. Census of India (2011), Directorate of Economics and Statistics, Ministry of Agriculture and Farmers Welfare, India Meteorological Department, Government of India.

*, ** & *** indicates 10, 5, and 1 percent level of significance

@Figure in the parenthesis represents (number of districts included in the state, total area of the state under ACZ), as per Census of India (2011) there are 640 districts in the country.

w includes illegal occupied J &K area by Pakistan and China.

$ Figures in the parentheses include percentage share of ACZ in the total geographical area of the country, i.e. 3,287,469 sq. km

P Figures in the parentheses includes percentage share of ACZ in the total Population of the country i.e. 1210854977 persons (Census, 2011).

DOI: https://doi.org/10.30564/jasr.v3i4.2269

ty, Trans-Gangetic Plains recorded the highest average foodgrain yield of 3.60 tones/ hectare.

Wide variations were observed in the distribution of rainfall across the zones. During the period 1966-2011, Eastern Himalayan Region (comprising north-eastern states and parts of West Bengal) followed by West Coast Plains & Ghats, have received the highest amount of annual rainfall whereas Western Dry Region and Trans-Gangetic Plains have received the lowest rainfall. Further, while rainfall registered an annual decline in the Himalayan regions and Gangetic Plains, it increased in Western and Southern Plateau & Hills and Coastal regions. The annual mean minimum temperature was the lowest in Western Himalayan Region comprising high altitude states of Himachal Pradesh, Jammu & Kashmir and Uttarakhand. On the other hand, East Coast Plains & Hills, Southern Plateau & Hills and Lower Gangetic Plains recorded the highest annual mean minimum temperature among the ACZs. Western Dry Region and Western Plateau & Hills had the highest mean maximum temperature. The estimates showed an increase in both the annual mean maximum and minimum temperature in all the ACZs with more pronounced changes in the minimum temperature. The increase in maximum temperature was significantly higher in Himalayan regions followed by Western Dry Region (parts of Rajasthan) and Central Plateau & Hills. On the other spectrum, the rate of increase in the minimum temperature was higher in both the Himalayan Regions followed by the Middle and Trans-Gangetic Plains indicating an accelerated warming during the period.

3. Data Sources

In this paper, a comprehensive district-level panel, on 301[①] districts spread across 14 agro-climatic zones was constructed for the period 1966-2011. The crop yields were paired with climate parameters (temperature and rainfall) and certain control variables to develop this large-scale panel which allows for inter-temporal and spatial assessment whilst controlling for district-specific factors and time trend. The data on area and production of crops and control factors like irrigated area, road length, literacy, tractors, pump sets and fertilizer consumption were compiled from the database maintained by International Crops Research Institute for the Semi-Arid Tropics (ICRISAT) under the Village Dynamics Studies in Asia (VDSA) project. Further, crops that were dominantly grown in the particular agro-climatic zone were purposely selected for assessment. The data on rainfall and temperature (minimum and maximum) were obtained from the India Meteorological Department (IMD), Government of India and later aggregated into the annual district metrics for the entire crop growing period. For the study, crop growing period is taken as a composite of sowing, germination and harvesting months for the respective crop.

4. Methodology

4.1 Method

There have been continuous methodological improvements for estimating the impact of climate variables (temperatures and rainfall) on agriculture production. Each method has been developed systematically to address some of the limitations of the former. In literature, three approaches have been widely used for analysing the economic effects of climate change on crop productivity: (1) Production function method, (2) Ricardian model, and (3) Panel data approach. Production function method, also known as crop modelling or agronomic-economic model, is a laboratory-type setup wherein under controlled experimental conditions, crops are exposed to a varied degree of climate scenarios and carbon dioxide levels, keeping farm level adaptations constant to study how change in rainfall, temperature and carbon dioxide precisely affect crops [36,37,38,39]. The Production function approach, however, does not reflect the farmer's adaptive behaviour to changing climatic conditions and thus it is likely to produce climate estimates that are downward biased [40]. In an alternative to crop simulation models, the cross-sectional Ricardian approach [41], which measures the impact of climate change on the net rent or value of agriculture land while integrating farmers' compensatory responses pertaining to the changes in both crop and input decisions. This method is similar to the hedonic price method of environmental valuation and explains regional differences in land values or productivity due to differences in climatic factors. However, the major lacuna with Ricardian approach is the omitted variable bias [40, 24]. This can occur if the critical farm variables (soil type, irrigation, and population density) correlated with climate is omitted from the regression model, leading to estimates that are not only biased but also inconsistent in nature. In the recent times, several researchers have used the panel data approach [42,40,24,26] to capture the effects of year-to-year change in climate variables on agriculture output by controlling for time-in-

① ICRISAT-VDSA database contains data for 311 districts spread across 19 states of India from 1966-67 to 2011-12 with 1966 base district boundaries. Due to different periodicity and paucity of data on certain variables and to create a balanced panel, a total of 301 districts were finally selected for the study.

 DOI: https://doi.org/10.30564/jasr.v3i4.2269

variant un-observables (e.g. soil and water quality) that may be correlated with climate and dependent variable, thereby reducing the possibility of an omitted variable bias. Also the spatial fixed effects capture region/ location specific time variant factors that may influence crop productivity [43]. Besides, with the panel data it is possible to account for short-term adaptations by the farmers in estimating the climate impact on agriculture productivity. Therefore, we used panel data approach to assess climate impact across different zones.

4.2 Empirical Specification

The present study used the following model specification to examine the impact of climate change on crop yields in each of the ACZ,

$$\log y_{dt} = c + \alpha_d + \partial t + \gamma log X_{dt} + \beta log\ W_{dt} + \varepsilon_{dt} \quad (1)$$

where y_{dt} represents crop yield, W_{dt} is a vector of climate variables (rainfall, maximum and minimum temperatures), X_{dt} denotesvector of controlvariables and ε_{dt} is the error term for the d^{th} district during the t^{th} time period, respectively. The model includes district level fixed effects, a_d which controls for unobserved district specific heterogeneity due to time-invariant factors that influence dependent variable. In their analysis, authors [40, 24, 44] all added entity fixed effects to eliminate the omitted variable bias. Further, a time trend has been incorporated in the model, as a proxy to absorb the technological effects and other farm level adaptations within an ACZ.

To ensure robustness of the applied panel regression, certain residual diagnostics were employed. We testedfor the first order autocorrelation in the residuals of a linear panel-data using the Woolridge test [45] of Homoscedasticity of error process across cross-sectional units was investigated through modified Wald test for group-wise heteroscedasticity [46]. Interestingly, with the application of the above procedures we found the presence of autocorrelation in most of the cases across the ACZs but there was no incidence of errors exhibiting group-wise heteroscedasticity. The latter may be attributed to the inclusion of trend component which corroborates with the findings of [45] and [45] of how incorporation of common trend in the panel imparts homogeneity across the cross-sectional units. Based on the above verifications, we applied feasible generalized least squares (FGLS) method with corrections for autocorrelation to estimate model (1) under the assumptions that; within panels, there is AR (1) autocorrelation and that the coefficient of the AR (1) process is common to all the panels. However, it is important to note that FGLSis feasible and tends to produce efficient and consistent estimates of standard errors, provided thatN < T that is panel time dimension, T, is larger than the cross-sectional dimension, N [49,50,51]. In our case, this assumption was satisfied as under each ACZ, the numbers of districts representing the cross-sectional units (N) were less than the time period.

4.3 Marginal Effects

The marginal effects of the climate parameters were calculated at their mean values from the regression coefficients. Under the model specification (1), the regression coefficients measure elasticity, i.e. proportionate change in crop yield to proportionate change in the independent variable. Hence, the combined marginal effect of climate variables, viz. rainfall, minimum and maximum temperature on crop yield was estimated using equation (2).

$$\frac{dy}{dc} = \left(\beta_{MT} * \left[\frac{\bar{Y}}{\overline{MT}} \right] + \beta_{MNT} * \left[\frac{\bar{Y}}{\overline{MNT}} \right] + \beta_R * \left[\frac{\bar{Y}}{\bar{R}} \right] \right) \quad (2)$$

Where, $\frac{dy}{dc}$ is combined marginal effect of change in climate variables on the crop yield, β denotes coefficients which are determined from the model, $\overline{MT}$ is mean maximum temperature, $\overline{MNT}$ is mean minimum temperature, $\bar{R}$ is mean rainfall, and $\bar{Y}$ is the mean crop yield during the period in an ACZ.

4.4 Future Climate Change Projections

The study used CORDEX South Asia multi-RCM reliability ensemble average estimate of projected changes in annual mean minimum and maximum temperature over India for the 30-year future periods: near-term (2016-2045), mid-term (2036-2065) and long-term (2066-2095) changes in future climate over India under RCPs 4.5and 8.5①scenarios relative to the base 1976-2005 to project the changes in crop yields [52]. In the near-term period, a similar increase of less than 2°Cin the mean minimum and maximum temperature was observed for both RCP4.5 and 8.5(Table 2).

① The Representative Concentration Pathways (RCPs) used by IPCC in its Fifth Assessment Report (AR5, 2014) describes the future trend in greenhouse gases concentration in the atmosphere due to human activities. The pathway delineates four future climate scenarios of RCP2.6, RCP4.5, RCP6.0 and RCP8.5, premised on different emission levels, energy use and socio-economic circumstances. For impact assessment we focused on RCPs 4.5 and 8.5 representing moderate and worst-case (business-as-usual) scenario.

DOI: https://doi.org/10.30564/jasr.v3i4.2269

Table 2. Projected changes annual mean minimum and maximum temperature over India

Variable				
Minimum temperature	Scenarios	Near-term (2030s)	Mid-term (2050s)	Long-term (2080s)
Maximum temperature	RCP 4.5	1.36 ± 0.18 (13.2%)	2.14 ± 0.28 (13.1%)	2.63 ± 0.38 (14.4%)
	RCP 8.5	1.50 ± 0.16 (10.7%)	2.60 ± 0.23 (8.8%)	4.43 ± 0.34 (7.7%)
	RCP 4.5	1.26 ± 0.20 (15.9%)	1.81 ± 0.27 (14.9%)	2.29 ± 0.36 (15.7%)
	RCP 8.5	1.36 ±0.16 (11.8%)	2.30 ±0.31 (13.5%)	3.94 ± 0.45 (11.4%)

Figure in the parenthesis indicate the associated uncertainty range

Source: Climate Change over India: An Interim report (2017). Centre for Climate Change Research, ESSO-IITM, Ministry of Earth Sciences, Govt. of India.

The mid-term warming in minimum temperature is projected to be in the range of 2.14 to 2.60°C while for the maximum temperature it is around 1.81 to 2.30°C.Under the RCP 4.5 minimum and maximum temperature surpasses 2°C by the end of the 21st century. In the far future minimum temperature is projected to increase beyond 4°C for RCP 8.5 with high degree of certainty. Overall, it is observed that the magnitude of changes in all India annual minimum temperature exceeds the changes estimated for the maximum temperature.

Further, a variation of 5, 10 and 12 percent in rainfall was assumed for the period of 2030s, 2050s and 2080sfor under the two scenarios. The direction of rainfall anomaly (positive or negative) for each of the ACZ was based on rainfall trend during the period from 2001-2011. The projected impactof climate change on crop yield expressed as percentage change was calculated using equation (3),

$$\Delta Y = \left(\frac{\partial Y}{\partial R}\right) * \Delta R + \left(\frac{\partial Y}{\partial T}\right) * \Delta T * 100 \quad (3)$$

Where, ΔY denotes change in crop yield, ΔR in rainfall and ΔT in temperature under and $\left(\frac{\partial Y}{\partial R}\right)$ and $\left(\frac{\partial Y}{\partial T}\right)$ are their marginal effects estimated from the model.

5. Results and Discussion

5.1 Marginal Effect and Projected Change for *kharif* Crop Yields

5.1.1 Marginal Effects

During the period from 1966-2011, a decline in rice yield was observed in nearly all the ACZs, with the highest reduction of 2.62 percent found in Eastern Himalayan Region (covering north-eastern states and parts of West Bengal). As shown in Table 3, maize yield declined in Central Plateau & Hills Western Dry Region, Trans-Gangetic Plainsand Upper Gangetic Plains by 1.33, 1.03, 0.65 and 0.03 percent, respectively. Regional variations are reflected from the fact that, while maize was negatively impacted by climatic variations in the above regions, it was benefitted in Himalayan Regions, Lower Gangetic Plains and Middle Gangetic Plains. The maximum reduction in groundnut occurred in Southern Plateau & Hills and West Coast Plains & Ghats, whereas in Central Plateau & Hills it showed an increase of 0.55 percent. Sorghum yield showed a decline of 4.54 percent in Central Plateau & Hills (covering parts of Madhya Pradesh, Rajasthan and Uttar Pradesh) and an increase of 4.68 percent in Western Plateau & Hills. The yield loss for sugarcane was to the extent of 9.91, 8.02 and 3.66 percent in East Coast Plains & Hills, Middle Gangetic Plains and Western Plateau & Hills, respectively. While Pearl millet yield showed an increase of 2.09 percent in Trans-Gangetic Plains, it registered a decline of 1.23 and 0.84 percent in Gujarat Plains & Hills and Western Dry Region. Finger millet increased by 1.10 percent in West Coast Plains & Ghats. Further, the effect of climatic variations has been found to be negative for cotton in Western Plateau & Hills and Trans-Gangetic Plains, where yield reduced by 1.74 and 0.59 percent.

5.1.2 Projected Impact under RCP 4.5

The climate projections showed that rice yield will decline by 5.49 and 6.79 percent in Eastern Himalayan Region by 2050s and 2080s. In near-term it is likely to reduce by 2.94 and 3.56 percent in Western and Eastern Himalayan Region. In case of both Eastern and Southern Plateau & Hills, rice yield will decline by about 1.7 percent by 2050s, respectively. By 2080s maize is likely to increase by around 7 to 8 percent in Western Himalayan Region and Lower Gangetic Plains. Yield loss in case of groundnut is expected to be around 5 percent by 2050s in Gujarat Plains & Hills. In near-term, groundnut yield will reduce by 1.96 and 1.82 percent in Southern Plateau & Hills and West Coast Plains & Ghats whereas, it will increase by 0.95 percent in Central Plateau & Hills. In the mid and long-term periods, sorghum is likely to increase around 8 and 11 percent in Western Plateau & Hills and decrease by the same magnitude in Central Plateau & Hills respectively. Cotton yieldwill decline the most in Western Plateau & Hills followed by Trans-Gangetic Plains. For sugarcane, yield is projected to decline by 11 and 13 percent in Middle Gangetic Plains (covering Bihar and parts of Uttar Pradesh) and East Coast Plains & Hills by 2030s. Pearl millet is likely to increase by 15.58 percent by mid-term

 DOI: https://doi.org/10.30564/jasr.v3i4.2269

Table 3. Regionally aggregated climate change impacts and projections for *kharif* crop yields(percent)

Agro-climatic Zone	Crops	Marginal Effects	With RCP 4.5 temperature projections			With RCP 8.5 temperature projections		
			2030s	2050s	2080s	2030s	2050s	2080s
			Δ MinT= 1.36	Δ MinT= 2.14	Δ MinT= 2.63	Δ MinT= 1.50	Δ MinT= 2.60	Δ MinT= 4.43
			Δ MaxT= 1.26	Δ MaxT= 1.81	Δ MaxT= 2.29	Δ MaxT= 1.36	Δ MaxT= 2.30	Δ MaxT= 3.94
			Δ R= (+/-) 5%	Δ R= (+/-) 10%	Δ R= (+/-) 12%	Δ R= (+/-) 5%	Δ R= (+/-) 10%	Δ R= (+/-) 12%
Western Himalayan Region	Rice	-2.34	-2.94	-4.41	-5.49	-4.02	-5.52	-9.59
	Maize	3.29	4.17	5.97	7.57	4.49	7.59	12.95
Eastern Himalayan Region	Rice	-2.62	-3.56	-5.49	-6.79	-3.89	-6.72	-11.39
	Maize	1.33	1.83	2.97	3.61	2.04	3.56	6.10
Lower Gangetic Plains	Rice	-1.17	-1.60	-2.34	-2.96	-1.71	-2.92	-4.87
	Maize	2.83	3.99	6.29	7.74	4.37	7.60	12.78
Middle Gangetic Plains	Rice	-0.17	-0.26	-0.41	-0.51	-0.28	-0.49	-0.80
	Maize	0.19	0.45	0.79	0.96	0.48	0.87	1.30
	Sugarcane	-8.02	-11.15	-17.43	-21.50	-12.21	-21.17	-35.70
Upper Gangetic Plains	Rice	-0.07	-0.16	-0.27	-0.33	-0.17	-0.30	-0.45
	Sugarcane	-0.13	-0.77	-1.57	-1.85	-0.82	-1.60	-2.18
	Maize	-0.03	0.12	0.27	0.32	0.12	0.25	0.27
	Sorghum	-0.68	-0.88	-1.36	-1.67	-0.97	-1.67	-2.91
Trans-Gangetic Plains	Rice	-0.37	-0.40	-0.54	-0.69	-0.44	-0.72	-1.30
	Cotton	-0.59	-0.86	-1.50	-1.78	-0.98	-1.74	-2.99
	Pearl Millet	2.09	8.43	15.58	18.90	8.63	16.49	22.03
	Maize	-0.65	-0.90	-1.53	-1.83	-1.03	-1.81	-3.14
Eastern Plateau & Hills	Rice	-0.67	-1.08	-1.71	-2.12	-1.16	-2.03	-3.27
	Maize	0.28	0.30	0.30	0.43	0.29	0.46	0.78
Central Plateau & Hills	Sorghum	-4.54	-5.71	-8.76	-10.80	-6.35	-10.87	-19.08
	Maize	-1.33	-1.75	-2.72	-3.35	-1.93	-3.33	-5.73
	Groundnut	0.55	0.95	1.59	1.94	1.03	1.84	2.95
Western Plateau & Hills	Sorghum	4.68	6.15	8.56	11.01	6.47	10.93	18.13
	Cotton	-1.74	-2.24	-3.36	-4.19	-2.45	-4.19	-7.18
	Sugarcane	-3.66	-4.39	-6.17	-7.84	-4.75	-7.97	-13.87
Southern Plateau & Hills	Rice	-0.72	-1.06	-1.65	-2.05	-1.14	-1.99	-3.27
	Groundnut	-1.56	-1.96	-3.06	-3.75	-2.19	-3.77	-6.62
East Coast Plains & Hills	Rice	-0.37	-0.57	-0.93	-1.13	-0.62	-1.09	-1.79
	Groundnut	-0.49	-0.52	-0.74	-0.93	-0.58	-0.97	-1.79
	Sugarcane	-9.91	-12.94	-20.26	-24.87	-14.37	-24.79	-42.87
West Coast Plains & Ghats	Rice	0.01	0.07	0.14	0.16	0.07	0.14	0.21
	Groundnut	-1.51	-1.82	-2.75	-3.39	-2.02	-3.44	-6.10
	Finger Millet	1.10	1.38	2.14	2.63	1.54	2.64	4.63
Gujarat Plains & Hills	Pearl Millet	-1.23	-2.00	-4.17	-4.70	-2.45	-4.54	-7.95
	Cotton	0.02	-0.30	-1.06	-1.08	-0.44	-0.95	-1.58
	Groundnut	-1.26	-2.31	-4.97	-5.58	-2.82	-5.31	-9.11
Western Dry Region	Pearl Millet	-0.84	-0.82	-1.17	-1.45	-0.95	-1.56	-3.01
	Maize	-1.03	-1.32	-2.03	-2.50	-1.46	-2.51	-4.37

Source: Authors estimation.

Note: Direction of rainfall for the future projections was premised on trend analysis for the period, 2001-2011.

period in Trans-Gangetic Plains. On the other hand, for the same period yield will reduce by 4.17 and 1.17 percent in Gujarat Plains & Hills and Western Dry Region.

5.1.3 Projected Impact under RCP 8.5

By the end of the century, maize yield is projected to increase by 12 percent in Western Himalayan Region and Lower Gangetic Plains. Under mid-term period, yield will lower by 3.33 and 2.51 percent in Central Plateau & Hills and Western Dry Region. In Western and Eastern Himalayan Region, rice yield is likely to reduce by 5.52 and 6.72 percent by 2050s, respectively. Rice yield in Lower Gangetic Plains is projected to decline by 4.87 percent by 2080s. Yield loss in case of Pearl millet by 2080s is expected to be around 7 and 3 percent in Gujarat Plains & Hills Western Dry Region respectively. The maximum decline in cotton yield was observed in Western Plateau & Hills, where yield is expected to decline by 4.19 and 7.18 percent under mid and long-term period. By 2050s, Finger millet yield will increase by 2.64 percent in West

DOI: https://doi.org/10.30564/jasr.v3i4.2269

Coast Plains & Ghats. By 2080s, sorghum is projected to decline up to 19 percent in Central Plateau & Hills. While on the other hand, for the similar period it will increase by about 18 percent in Western Plateau & Hills. In Middle Gangetic Plains and East Coast Plains & Hills, sugarcane yield is expected to decline by 21.17 and 24.79 percent under mid-term period, respectively. The yield of ground is projected to decline by 9.91 and 6.62 percent in Gujarat Plains & Hills and Southern Plateau & Hills by 2080s, respectively.

5.2 Marginal Effect and Projected Change for *rabi* Crop Yields

5.2.1 Marginal Effects

As shown in Table 4, marginal effect of climate variables

Table 4. Regionally aggregated climate change impacts and projections for *rabi* crop yields(percent)

Agro-climatic Zone	Crops	Marginal Effects	With RCP 4.5 temperature projections			With RCP 8.5 temperature projections		
			2030s	2050s	2080s	2030s	2050s	2080s
			Δ MinT= 1.36	Δ MinT= 2.14	Δ MinT= 2.63	Δ MinT= 1.50	Δ MinT= 2.60	Δ MinT= 4.43
			Δ MaxT= 1.26	Δ MaxT= 1.81	Δ MaxT= 2.29	Δ MaxT= 1.36	Δ MaxT= 2.30	Δ MaxT= 3.94
			Δ R= (+/-) 5%	Δ R= (+/-) 10%	Δ R= (+/-) 12%	Δ R= (+/-) 5%	Δ R= (+/-) 10%	Δ R= (+/-) 12%
Western Himalayan Region	Wheat	-0.47	-0.66	-1.05	-1.29	-0.73	-1.27	-2.14
	Barley	-0.76	-0.91	-1.25	-1.60	-0.98	-1.63	-2.81
Eastern Himalayan Region	Wheat	-2.03	-2.61	-3.98	-4.93	-2.87	-4.93	-8.49
	Rapeseed & Mustard	-1.08	-1.44	-2.16	-2.70	-1.56	-2.68	-4.53
Lower Gangetic Plains	Wheat	-0.96	-1.04	-1.45	-1.83	-1.14	-1.90	-3.43
	Rapeseed & Mustard	-1.21	-1.67	-2.46	-3.10	-1.79	-3.06	-5.12
Middle Gangetic Plains	Wheat	-0.28	-0.37	-0.56	-0.69	-0.40	-0.69	-1.18
	Rapeseed & Mustard	1.04	1.26	1.90	2.36	1.39	2.38	4.15
	Barley	0.04	0.05	0.10	0.12	0.06	0.12	0.22
Upper Gangetic Plains	Wheat	-0.09	-0.11	-0.17	-0.21	-0.12	-0.21	-0.37
	Barley	0.01	0.03	0.06	0.08	0.03	0.06	0.08
	Rapeseed & Mustard	0.20	0.29	0.46	0.57	0.32	0.56	0.91
Trans-Gangetic Plains	Wheat	-1.02	-1.53	-2.57	-3.11	-1.70	-3.01	-5.02
	Barley	-0.26	-0.30	-0.40	-0.52	-0.32	-0.54	-0.95
	Rapeseed & Mustard	1.59	2.32	3.89	4.70	2.59	4.58	7.71
Eastern Plateau & Hills	Wheat	-0.26	-0.30	-0.48	-0.58	-0.34	-0.59	-1.07
	Linseed	-0.87	-1.23	-2.00	-2.43	-1.36	-2.39	-4.04
Central Plateau & Hills	Wheat	-0.94	-1.31	-2.07	-2.54	-1.44	-2.50	-4.22
	Rapeseed & Mustard	2.73	3.69	5.76	7.10	4.06	7.03	11.97
Western Plateau & Hills	Wheat	-0.88	-1.12	-1.62	-2.05	-1.21	-2.05	-3.49
	Rapeseed & Mustard	-1.86	-2.05	-2.45	-3.29	-2.13	-3.44	-6.01
Southern Plateau & Hills	Wheat	-1.27	-1.73	-2.62	-3.27	-1.88	-3.23	-5.44
	Linseed	-1.35	-1.72	-2.51	-3.16	-1.86	-3.16	-4.88
East Coast Plains & Hills	Wheat	-1.46	-2.01	-3.19	-3.92	-2.22	-3.86	-6.56
	Rapeseed & Mustard	3.45	4.71	7.41	9.10	5.19	8.99	15.31
West Coast Plains & Ghats	Wheat	0.33	0.48	0.77	0.95	0.54	0.92	1.54
	Rapeseed& Mustard	2.45	3.37	6.34	6.53	3.71	7.47	10.91
Gujarat Plains & Hills	Wheat	0.44	1.29	3.20	3.49	1.62	3.20	5.29
	Rapeseed & Mustard	0.31	0.86	2.13	2.32	1.09	2.14	3.56
Western Dry Region	Wheat	-2.73	-3.71	-5.84	-7.17	-4.09	-7.03	-12.05
	Rapeseed & Mustard	2.57	3.50	5.50	6.75	3.86	6.69	11.42

Source: Authors estimation

Note: Direction of rainfall for the future projections was premised on trend analysis for the period, 2001-2011.

 DOI: https://doi.org/10.30564/jasr.v3i4.2269

on wheat yield was found to be negative in all the growing regions except West Coast Plains & Ghats and Gujarat Plains & Hills. The maximum reduction in wheat yield was observed in Western Dry Region (2.73 percent) and Eastern Himalayan Region (2.03 percent). On the other hand,yield of barley showed a decline of 0.76 and 0.26 percent in Western Himalayan Region and Trans-Gangetic Plains, whereas in Middle and Upper Gangetic Plains, it registered a marginal increase of 0.04 and 0.01 percent. In nearly all the growing regions, rapeseed & mustard was positively impacted reflecting high tolerance and resilience of crop to the changing climatic conditions. In East Coast Plains & Hills, Central Plateau & Hills and Western Dry Region, rapeseed & mustard yield showed the maximum increase of 3.45, 2.73 and 2.57 percent respectively. On the other spectrum, yield reduced by 1.86 and 1.21 percent in Western Plateau & Hills and Lower Gangetic Plains. During the period, linseed yield declined by 1.35 and 0.87 percent in both the Eastern and Southern Plateau & Hills respectively.

5.2.2 Projected Impact under RCP 4.5

Climate projections for *rabi* crops indicate that by 2050s and 2080s wheat yield will reduce by 5.84 and 7.17 percent in Western Dry Region. For the similar periods it will reduce by 3.98 and 4.93 percent in Eastern Himalayan Region and 2.57 and 3.11 percent in Trans-Gangetic Plains. In Gujarat Plains & Hills, wheat yield is likely to increase by 3.20 percent by 2050s. Rapeseed & mustard is projected to increase up to 9.10, 7.10 and 6.75, percent by 2080s in East Coast Plains & Hills, Central Plateau & Hills and Western Dry Region. By 2050s, barley yield will reduce by 1.25 and 0.4 percent in Western Himalayan Region and Trans-Gangetic Plains.

5.2.3 Projected Impact under RCP 8.5

By 2080s, wheat yield is projected to decline by 12.05, 8.49 and 6.56 percent in Western Dry Region, Eastern Himalayan Region and East Coast Plains & Hills, respectively. InTrans-GangeticPlains wheat yield will be lower by 3.01 percent under the mid-term period. Barley was not much impacted to climate change, as yield loss were projected to be 0.54 and 1.63 percent by 2050s,in Trans-Gangetic Plains and Western Himalayan Region. For the long-term period, rapeseed & Mustard yield is expected to increase by around 11-12 percent in Central Plateau & Hills, West Coast Plains & Ghats and Western Dry Region. In Eastern Plateau & Hills and Southern Plateau & Hills, linseed yield is expected to decline by 2.39 and 3.16 percent by 2050s.

6. Conclusion

The study made an attempt to examine the large-scale heterogeneity across the Indian landscape by capturing the idiosyncrasy of ACZs and understanding the sensitivity of major *kharif* and *rabi* crop yields to climate change at a spatially disaggregated level. An examination of spatio-temporal change in temperature revealed a rise in both the annual mean maximum and minimum temperature, with more pronounced changesobserved in annual mean minimum temperature across the ACZs. The empirical results indicate progressive reduction in most of the crop yields,but the magnitude impacts and projections vary by ACZs.The changes in crop yields projected under RCP 8.5 were more pronounced compared to RCP 4.5; largely due to higher temperature projections under the former.The results indicate that the direct and near-term impact of climate change on crop yields will be smaller as compared to mid and long-term projections. Thus the study suggests that there is a dire need to formulate region-specific interventions and adaptation strategies to maintain food security and livelihood protection of farmersin the respective region. Concerted efforts are needed in development and dissemination of climate resilient varieties and on-farm management practices, promotion of integrated watershed management which includes up-scaling techniques such as solar pumps, drip irrigation and sprinklers for greater water use efficiency. Improved awareness, communication andtraining regarding micro-level sensitivity to climate induced perturbations in conjunction with insurance covers across regionsis crucial for desired changes in farming practices. As climate becomes more unpredictable, opportunities for diversification to non-farm activities becomes essential for reducing exposure to livelihood shocks. From policy perspective, mainstreaming climate adaptation in the rural developmental paradigm is imperative to improve the envisaged agriculture outputs and outcomes. The long-term essentiality for regional planning arises from the need for a framework that would act as a stabilizer, addressing regional imbalances and ensuring intergenerational equity in resource use.

Our main interest through this study was to understand the spatial distribution of climate impact on crop yields. However, the results of this study needs to be interpreted with caution because of certain limitations. First, the sensitivity of crop yields to changes in climate variables was examined, assuming linear climate-crop yield relation which might not be true under certain conditions. Moreover, such an assumption ignores the incremental impact of climate parameters on crop yields.

DOI: https://doi.org/10.30564/jasr.v3i4.2269

There are studies that show non-linearity between climate variables and crop yields [53, 24]. Second, due to unavailability of future climate estimates at agro-climatic zone level, our projections assume uniform changes in rainfall and temperature across the zones. However, climate variations differ across regions, and thus may influence the nature of climate change projections on crop yields.

References

[1] IPCC. Summary for Policymakers. In: Global Warming of 1.5°C. Masson-Delmotte, V., P. Zhai, H.-O. Pörtner, D. Roberts, J. Skea, P.R. Shukla, A. Pirani, W. Moufouma-Okia, C. Péan, R. Pidcock, S. Connors, J.B.R. Matthews, Y. Chen, X. Zhou, M.I. Gomis, E. Lonnoy, T. Maycock, M. Tignor, & T. Waterfield (Eds.)], World Meteorological Organization, Geneva, Switzerland, 2018.

[2] Lobell, D.B., Field, C.B. Global scale climate-crop yield relationships and the impacts of recent warming. Environmental Research Letters, 2007, 2(1): 014002.

[3] Nelson, G.C., Rosegrant, M.W., Koo, J., Robertson, R., Sulser, T., Zhu, T., Ringler, C., Msangi, S., Palazzo, A., Batka, M., &Magalhaes, M. Climate change: impact on agriculture and costs of adaptation. International Food Policy Research Institute, Washington, DC, 2009.

[4] Lobell, D.B., Schlenker, W., Costa-Roberts, J. Climate trends and global crop production since 1980. Science, 2011, 333(6042): 616-620.

[5] Mishra, A., Singh, R., Raghuwanshi, N.S., Chatterjee, C., Froebrich, J. Spatial variability of climate change impacts on yield of rice and wheat in the Indian Ganga Basin. Science of the Total Environment, 2013, 468: 132-138.

[6] Mall, R.K., Singh, R., Gupta, A., Srinivasan, G., Rathore, L.S. Impact of climate change on Indian agriculture: A review. Climatic Change, 2006, 78(2-4): 445-478.

[7] Aggarwal, P.K. Global climate change and Indian agriculture: impacts, adaptation and mitigation. Indian Journal of Agricultural Sciences, 2008, 78(11): 911-919.

[8] Falkenmark, M., Rockström, J., Karlberg, L. Present and future water requirements for feeding humanity. Food security, 2009, 1(1): 59-69.

[9] Nelson, G. C., Rosegrant, M. W., Palazzo, A., Gray, I., Ingersoll, C., Robertson, R., Tokgoz, S., Zhu, T., Sulser, T., Ringler, C. Food Security, Farming and Climate Change to 2050. Research Monograph, International Food Policy Research Institute, Washington, DC, 2010.

[10] Singh, P., Singh, N., Nedumaran, S., Bantilan, C., Byjesh, K. Evaluating adaptation options at crop level for climate change in the tropics of south Asia and west Africa. In: Climate Change Challenges and Adaptations at Farm-level: Case Studies from Asia and Africa, Eds: N. P. Singh, C. Bantilan, K. Byjesh, and S. Nedumaran. CABI Private Limited, 2015, 115-137.

[11] FAO, 2016.

[12] Gornall, J., Betts, R., Burke, E., Clark, R., Camp, J., Willett, K., Wiltshire, A. Implications of climate change for agricultural productivity in the early twenty-first century. Philosophical Transactions of the Royal Society B: Biological Sciences, 2010, 365(1554): 2973-2989.

[13] Porter, J.R. et al. Food security and food production systems. In: Climate change 2014: impacts, adaptation, and vulne*rabi*lity. Part A: global and sectoral aspects (C.B. Field, V.R. Barros, D.J.

[14] Kothawale, D.R., Rupa Kumar, K. On the recent changes in surface temperature trends over India. Geophysical Research Letters, 2005, 32(18).

[15] Kothawale, D.R., Munot, A.A., Kumar, K.K. Surface air temperature variability over India during 1901-2007, and its association with ENSO. Climate Research, 2010, 42(2): 89-104.

[16] Rao, B.B., Chowdary, P.S., Sandeep, V.M., Rao, V.U.M., Venkateswarlu, B. Rising minimum temperature trends over India in recent decades: implications for agricultural production. Global and Planetary Change, 2014, 117: 1-8.

[17] Mondal, A., Khare, D., Kundu, S. Spatial and temporal analysis of rainfall and temperature trend of India. Theoretical and applied climatology, 2015, 122(1-2): 143-158.

[18] Kumar, V., Jain, S.K., Singh, Y. Analysis of long-term rainfall trends in India. Hydrological Sciences Journal-Journal des Sciences Hydrologiques, 2010, 55(4): 484-496.

[19] Jayaraman, T., Murari, K. Climate change and agriculture: Current and future trends, and implications for India. Review of Agrarian Studies, 2014, 4(1): 1-49.

[20] Goswami, B.N., Venugopal, V., Sengupta, D., Madhusoodanan, M.S., Xavier, P.K., Increasing trend of extreme rain events over India in a warming environment. Science, 2006 314(5804): 1442-1445.

[21] Jain, S.K., Kumar, V. Trend analysis of rainfall and temperature data for India. Current Science, 2012, 37-49.

 DOI: https://doi.org/10.30564/jasr.v3i4.2269

[22] Acharya, S.S. Sustainable agriculture and rural livelihoods. Agricultural Economics Research Review, 2006, 19(2): 205-217.

[23] Jain, M., Naeem, S., Orlove, B., Modi, V., DeFries, R.S. Understanding the causes and consequences of differential decision-making in adaptation research: adapting to a delayed monsoon onset in Gujarat, India. Global Environmental Change, 2015, 31: 98-109.

[24] Guiteras R. The impact of climate change on Indian agriculture. Manuscript, Department of Economics, University of Maryland, College Park, Maryland, 2009.

[25] Kumar, S.N., Aggarwal, P.K., Rani, D.S., Saxena, R., Chauhan, N., Jain, S. Vulne*rabi*lity of wheat production to climate change in India. Climate Research, 2014, 59(3): 173-187.

[26] Birthal, P.S., Khan, T.M., Negi, D.S., Agarwal, S. Impact of climate change on yields of major food crops in India: implications for food security. Agricultural Economics Research Review, 2014a, 27 (347-2016-17126): 145-155.

[27] Cline, W. Global Warming and Agriculture: Impact Estimates by Country, Washington, DC, 2007.

[28] Mall, R.K., Singh, R., Gupta, A., Srinivasan, G., Rathore, L.S. Impact of climate change on Indian agriculture: a review. Climatic change, 2006, 78(2-4): 445-478.

[29] Aggarwal, P.K. Vulne*rabi*lity of Indian agriculture to climate change: current state of knowledge, paper presented at the National Workshop - Review of Implementation of Work Programme towards Indian Network of Climate Change Assessment, Ministry of Environment and Forests, New Delhi, 2009,

[30] Singh, N.P., Bantilan, C., Byjesh, K. Vulne*rabi*lity and policy relevance to drought in the semi-arid tropics of Asia-A retrospective analysis. Weather and Climate extremes, 2014, 3: 54-61.

[31] Singh, N.P., Anand, B., Singh, S., Khan, A. Mainstreaming climate adaptation in Indian rural developmental agenda: A micro-macro convergence. Climate Risk Management, 2019, 24: 30-41.

[32] Government of India. Agro-climatic regional planning: an overview, Planning Commission, New Delhi, 1989.

[33] Basu, D.N., Guha, G.S. Agro-climatic Regional Planning in India,1996.

[34] Singh, R.K., Singh, D.N. An agroclimatic approach to agricultural development in India. In: Systems approaches for agricultural development, Eds: de VriesF.P., Teng P., Metselaar K. Springer, Dordrecht. 1993: 111-125.

[35] Chand, M., Puri, V.K. Regional planning in India (Vol.1). Allied Publishers, 1983.

[36] Rosenzweig, C., Parry, M.L. Potential impact of climate change on world food supply. Nature, 1994, 367(6459): 133-138.

[37] Rao, D.G., Sinha,S.K. Impact of Climate Change on Simulated Wheat Production in India.In: Implications of Climate Change for International Agriculture: Crop Modelling Study (Rosenzweig C, Iglesias A eds), US Environmental Protection Agency, Washington, 1994.

[38] Lal, M., K.K. Singh, L.S. Rathore, G. Srinivasan and S.A. Saseendran. Vulne*rabi*lity of Rice and Wheat Yields in North-West India to Future Changes in Climate. Agriculture and Forest Meteorology, 1998, 89: 101-114.

[39] Mathauda, S.S., H.S. Mavi, B.S. Bhangoo, B.K. Dhaliwal. Impact of Projected Climate Change on Rice Production in Punjab (India). Tropical Ecology, 2000, 41(1): 95-98.

[40] Deschênes, O., Greenstone, M. The economic impacts of climate change: evidence from agricultural output and random fluctuations in weather. American Economic Review, 2007, 97(1): 354-385.

[41] Mendelsohn, R., Nordhaus, W., Shaw, D. The impact of global warming on agriculture: a Ricardian analysis. American Economic Review, 1994, 84: 753-771.

[42] Kelly, D.L., Kolstad, C.D., Mitchell, G.T. Adjustment costs from environmental change. Journal of Environmental Economics and Management, 2005, 50(3): 468-495.

[43] Birthal, P.S., Negi, D.S., Kumar, S., Aggarwal, S., Suresh, A., Khan, M. How sensitive is Indian agriculture to climate change?. Indian Journal of Agricultural Economics, 2014b, 69(902-2016-68357): 474-487.

[44] Kala, N., Kurukulasuriya, P., Mendelsohn, R. The impact of climate change on agro-ecological zones: evidence from Africa. Environment and Development Economics, 2012, 17(6): 663-687.

[45] Wooldridge, J. M. Econometric Analysis of Cross Section and Panel Data. Cambridge, MA: MIT Press, 2002.

[46] Greene, W. Econometric Analysis. Upper Saddle River, NJ: Prentice-Hall, 2000.

[47] Banerjee, A. Panel Data Unit Roots and Cointegration: An Overview, Oxford Bulletin of Economics and Statistics, 1999, Special Issue 035-9049.

[48] Nelson, M., Donggyu S. A. Computationally Simple Cointegration Vector Estimator for Panel Data, Department of Economics working Papers, The Ohio

  DOI: https://doi.org/10.30564/jasr.v3i4.2269

State University, 2001.
[49] Kmenta, J. Elements of Econometrics. 2nd ed. New York: Macmillan, 1986.
[50] Beck, N., Katz, J.N. What to do (and not to do) with time-series cross-section data. American political science review, 1995, 89(3): 634-647.
[51] Hoechle, D. Robust standard errors for panel regressions with cross-sectional dependence. The Stata journal, 2007, 7(3): 281-312.
[52] Ministry of Earth Sciences (MoES). Climate Change over India: An Interim Report, Eds. Krishnan R., and Sanjay J. ESSO-Indian Institute of Tropical Meteorology, Ministry of Earth Sciences, Government of India, Pune, 2017.
[53] Schlenker, W., Roberts, M. Nonlinear effects of weather on crop yields: implications for climate change. Review of Agricultural Economics, 2006, 28.

 DOI: https://doi.org/10.30564/jasr.v3i4.2269

BILINGUAL PUBLISHING CO.
Pioneer of Global Academics Since 1984

Journal of Atmospheric Science Research
https://ojs.bilpublishing.com/index.php/jasr

ARTICLE

Corona with Streamers in Atmospheric Pressure Air in a Highly Inhomogeneous Electric Field

Victor Tarasenko* **Evgenii Baksht** **Vladimir Kuznetsov** **Victor Panarin** **Victor Skakun** **Eduard Sosnin** **Dmitry Beloplotov**

Institute of High Current Electronics, Siberian Branch (SB), Russian Academy of Sciences (RAS), 2/3 Akademicheskii Ave., Tomsk, 634055, Russia

ARTICLE INFO

Article history
Received: 2 September 2020
Accepted: 7 September 2020
Published Online: 30 September 2020

Keywords:
Positive and negative coronas
Atmospheric pressure air
Highly inhomogeneous electric field
ICCD camera
Ball streamer
Cylindrical streamer

ABSTRACT

The paper presents research data on positive and negative coronas in atmospheric pressure air in a highly inhomogeneous electric field. The data show that irrespective of the polarity of pointed electrodes placed in a high electric field (200 kV/cm), this type of discharge develops via ball streamers even if the gap voltage rises slowly (0.2 kV/ms). The start voltage of first positive streamers, compared to negative ones, is higher and the amplitude and the frequency of their current pulses are much lower: about two times and more than two orders of magnitude, respectively. The higher frequency of current pulses from negative streamers provides higher average currents and larger luminous areas of negative coronas compared to positive ones. Positive and negative cylindrical streamers from a pointed to a plane electrode are detected and successive discharge transitions at both polarities are identified.

1. Introduction

Corona discharges in air and other gases at different pressures continue to attract the attention of researchers [1-25]. Coronas are a self-sustained discharge arising near an electrode or electrodes with a small radius of curvature [26,27]. Typically, two main areas appear in this type of discharge: an ionization region near a pointed electrode where the electric field is high and a region remote from it where the field is low and the current is provided by charged particle drift. As has recently been proven [28], the part of current in non-ionized region is contributed by dynamic displacement current due to fast plasma expansion by streamers from a pointed electrode. Corona discharges can be initiated by applying DC and AC voltages and by applying short voltage pulses which make them short-lived in a single form [5,7,13].

Coronas can be positive or negative depending on the voltage polarity of pointed electrodes [1-27]. Negative coronas can produce current pulses hundred nanoseconds long whose frequency increases with voltage [26,27]. Such corona bursts are known as Trichel pulses [29], and in some studies, they are related to negative streamers [18,20,24]. Data are also available on how this type of discharge near a negative electrode is

**Corresponding Author:*
Victor Tarasenko,
Institute of High Current Electronics, Siberian Branch (SB), Russian Academy of Sciences (RAS), 2/3 Akademicheskii Ave., Tomsk, 634055, Russia;
Email: VFT@loi.hcei.tsc.ru

DOI: https://doi.org/10.30564/jasr.v3i4.2342

transformed and constricted [4]. Positive coronas can produce cylindrical jets [7] whose length increases greatly if an additional ring electrode is present in their region [22]. The threshold current for corona-to-glow and glow-to-spark transitions can vary with the geometry of an anode, its resistivity, length of gap, and gas flow [3]. The start voltage of positive coronas, compared to negative ones, is higher [4,20,26,27].

Despite abundant research data on corona discharges, their studies are continued [17-25,30]. In particular, some features of coronas remain unclear. For example, if the gap voltage rises slowly, lower voltages are needed for a negative corona [4,20]. At the same time, the electric field needed for a negative streamer is about twice that for a positive one: ~10 kV/cm^2 against 5 kV/cm^2 in atmospheric pressure air [27]. Thus, the question arises of why corona discharges appear earlier at negative polarity and cylindrical streamers at positive. This and other features of corona discharges are still poorly understood. From the available data, it is unclear whether the first current pulses of negative and positive coronas can be related to the formation of streamers.

Only recently [20,30] it has been found that the initiation of corona discharges can start with the formation of a streamer with a large diameter at both voltage polarities. Such streamers propagated from needle electrodes with a tip radius of tens of microns at a slowly rising voltage [20, 30]. Note that in some studies [31,32], such streamers produced by nanosecond voltage pulses were termed broad or wide, and they were really wide, reaching 8 cm in diameter at high rates of rise of voltage ($dU/dt > 10^{14}$ kV/ns).

All the foregoing suggests that further research in the features of coronas is needed. In the paper presented, we analyze the initiation of corona discharges from electrodes with a small radius of curvature in point-plane gaps and the conditions for their transition to other forms at both voltage polarities with a minimal voltage of less than 2 kV.

2. Experimental Setup and Measuring Techniques

The experimental setup for research in corona discharges in atmospheric pressure air comprised a power supply, a point-plane electrode gap, and a measuring system (Figure 1).

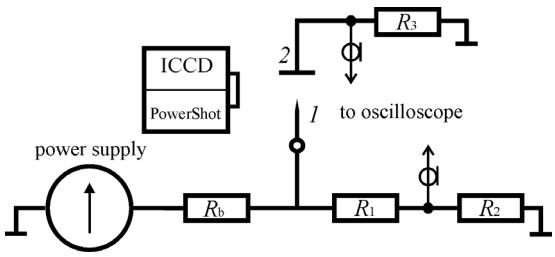

Figure 1. Experimental setup: R_b = 18 MOhm, R_1 = 2.5 MOhm, R_2 = 2.5 kOhm, R_3 = 1 kOhm

For assessing the minimum start voltage of coronas, we used a high-voltage source with a voltage stability and long needles with a small radius of curvature (Table 1).

Table 1. Needle parameters

Size	Diameter, mm	Tip radius, μm
No. 1a	0.32	11-13
No. 1b	0.32	40
No. 2	0.61	30
No. 3	1.04	100
No. 4	3	200

Most of the experiments were performed with a beading needle of size No. 1a having a tip radius of 11-13 μm, length of 55 mm, and diameter of 0.32 mm. Because the tip of needle No. 1a during high-voltage operation was melted and its radius increased up to ≈40 μm (needle No. 1b), the needle was regularly replaced by a fresh one. The tips of the other needles (Nos. 2, 3, 4) after spark breakdowns were less eroded but their radius was also increased. The least increase in the tip radius was observed for needle No. 4. The material of needle No. 4 was copper, and that of needles Nos. 1, 2, 3 was stainless steel.

The second (grounded) electrode was plane, allowing current measurements. The distance between the tip of a needle and plane electrode was varied from 2 to 50 mm. Because needle No. 1a was subjected to strong corona vibrations due to its small dimeter and large length, its tip was fixed with a teflon plate to reliably capture the discharge form. Several experiments were performed only with a needle (and with no shunt) for which all grounded metal conductors were spaced from it by more than 10 cm.

In our experiments, we used three voltage sources: (1) a source with a stabilized voltage of 0.4- 5 kV accurate to no worse than 0.2% and with a rate of voltage rise no greater than 0.2 kV/ms; (2) a source with a voltage of up to 36 kV and rate of voltage rise of no more than 0.2 kV/ms; (3) and a source with sinusoidal voltage pulses of both polarities rising up to 20 kV in ≈500 ns.

The form of corona discharges was captured in frame-by-frame mode with a Canon PowerShot SX 60 HS camera and was recorded with an HSFC PRO four-channel ICCD camera at a minimum frame duration of 3 ns.

The time dependence of voltage was traced with a high-voltage probe and a Tektronix TDS 3034 oscilloscope. The discharge current measured by a high-resistance shunt (R = 1 kOhm) was recorded with a resolution of no worse than 5 ns. Thus, we could measure the pulsed and steady component of the current through the gap. All experiments were performed in a laboratory room in am-

 DOI: https://doi.org/10.30564/jasr.v3i4.2342

bient air at a temperature of ≈20 °C and humidity of no more than 60%.

3. Experimental Results

3.1 Current-voltage Characteristics of Corona Discharges

Despite numerous experimental studies of corona discharges, no complex analysis is available to judge their evolution. In particular, little is known about the early stage of coronas, the more so as their studies with high time resolution are comparatively rare. In our study, we have analyzed the relationship between the characteristics of coronas and modes of their operation. Figure 2 shows the average discharge current versus the voltage of both polarities at the tip of needle No. 4.

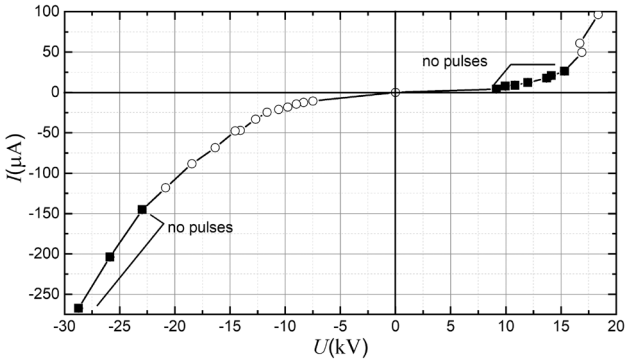

Figure 2. Average discharge current versus negative and positive polarity voltage with needle No. 4 spaced from plane electrode by 20 mm

Needle No. 4 was used because its tip was little affected by several sparks while the tips of needles Nos. 1, 2, 3 were blunted. The average current was determined through oscilloscope measurements for 400 μs. Each point in Figure 2 was obtained at constant voltage. During the measurement time (400 μs), short current pulses were recorded (open circles on the diagram). At the same voltage level, their frequency at negative polarity was more than an order of magnitude greater than its value at positive polarity. Thus, the discharge current on the diagram is represented by its quasi-steady and pulsed components.

The current-voltage characteristics in Figure 2 are typical for corona discharges: higher discharge start voltages and lower average discharge currents at positive than at negative voltage polarity. The oscilloscope recorded the corona current and the gap voltage simultaneously at each measurement point, allowing us to identify pulsed, quasi-steady, and mixed modes of the current flow at each voltage (by varying the time sweep) and to determine the frequency of current pulses, their amplitude, and duration.

The pulsed mode was always observed at initiation of corona discharge. Previous studies showed that the pulsed mode is related with the formation of spherical (wide) streamers in the vicinity of a needle [20].

At both voltage polarities, a quasi-steady discharge mode (free of individual pulses during 400 μs) was observed. At positive polarity, the voltage for this mode was relatively lower than at negative polarity. Over time, the quasi-steady mode transformed to a mixed one. This mode comprised two components: quasi-steady and pulsed. At positive polarity, the contribution from individual pulses to the mixed mode was negligible. At negative polarity, such a mode with its quasi-steady component and Trichel pulses [26,29] was observed with increasing voltage after the start of a corona. For negative polarity, the voltage at which current pulses with a relatively high frequency appeared was about 7.5 kV (Figure 2). For positive polarity, it was higher. When voltage of any polarity was increased greatly, the corona transformed to a glow and then to a spark discharge.

The waveforms of voltage and current were recored not only at constant voltages but also at voltage rise time and fall time from tens of milliseconds to several seconds. As for the average corona current, the current-voltage characteristics at relatively short voltage rise and fall times differed little from those at constant voltages. However, it was possible to observe all modes and transitions of corona discharge.

Figure 3 shows the waveforms of voltage and current of a negative corona recorded within 35 ms when applying needle No. 1b.

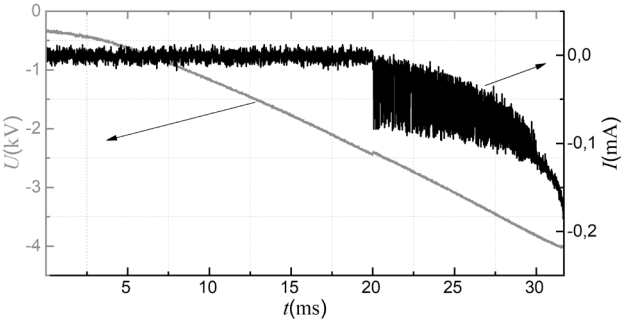

Figure 3. Waveforms of voltage and current of negative corona recorded from within ~35 ms. Needle No. 1b. Length of gap 3 mm

Until ≈20 ms (Figure 3), the current through the gap was low (<1 μA) and corresponded to dark current due to air ionization by high-energy cosmic particles [27]. Once a negative corona was ignited (≈2.2 kV), Trichel pulses and then quasi-steady component appeared. The quasi-steady component increased with increasing the voltage while the amplitude of current pulses decreased (if counted from the quasi-steady level) such that they became undetectable

DOI: https://doi.org/10.30564/jasr.v3i4.2342

at ≈3.1 kV. We think that it is the onset of corona-to-glow discharge transition. The transition was accompanied by electron emission from a bright cathode spot and gradual extension of the corona current-voltage characteristic into a glow one. Further increasing the voltage gave rise to a spark discharge such that the gap voltage dropped and the current increased significantly. Transforming the spark to a corona or a glow discharge required a decrease in the power supply voltage. All these modes can be judged from their respective waveforms and images in the sections below.

Figure 4 shows the waveforms of voltage and current of a positive corona when applying needle No. 1b. When the needle was positive, the current got quasi-steady after the first pulse and remained quasi-steady during >400 μs. The mixed mode was observed only at relatively high voltages.

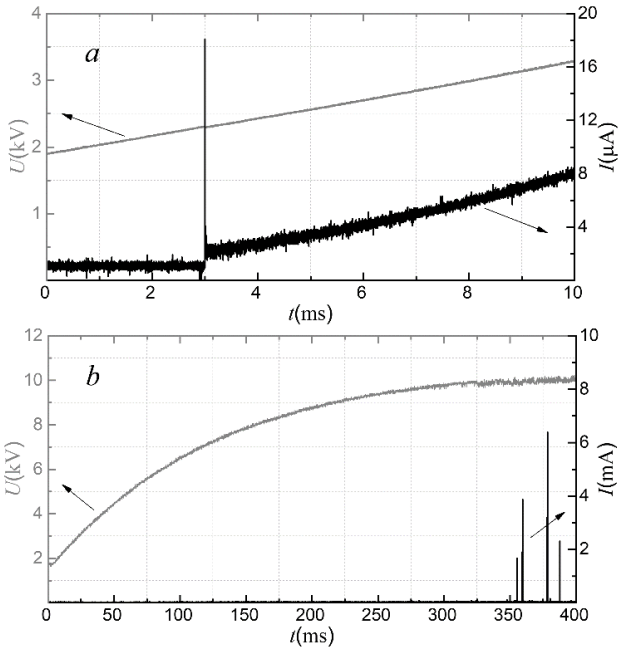

Figure 4. Waveforms of voltage and current of positive corona when applying needle No. 1b. Length of gap 10 mm

The positive corona developed via ball streamers. The appearance of the ball streamer in the vicinity of the needle tip is accompanied by a short current pulse (Figure 4a) after which the discharge became quasi-steady and its average current increased with increasing the voltage. In the quasi-steady mode, pulses were also possible but their frequency was too low to make them full-blown. The high amplitude of the current pulse is due to the high rate of ionization processes in the vicinity of the needle tip, where the electric field strength is very high. The short duration of the current pulse is caused by a rapid decrease in the rate of ionization processes as the diameter of the streamer increases and the strength of the electric field at its front decreases. These features of current during the development of a streamer were studied in [28].

At a higher voltage (≈10 kV, Figure 4b), the positive corona revealed cylindrical streamers [30]. As can be seen in Figure 4b, cylindrical streamers are also accompanied by current pulses. Their amplitude and duration are greater than that for the ball streamers formed in the vicinity of the needle tip at lower voltages. The voltage practically does not change. It drops when the discharge transforms to a spark with increasing the power supply voltage. As has been shown [26], lower values of slowly rising voltage in an inhomogeneous electric field are needed for a spark breakdown from positive pointed electrodes compared to negative ones. Our study confirms this conclusion (Figure 2).

3.2 Initiation of Coronas

Let us look closer at the initiation of corona discharges. Our previous studies [20,30] show that the initiation of a corona starts with a ball streamer not only at negative but also at positive voltage polarity. In particular, such a streamer is identified from current pulses with a duration of 100-200 ns recorded by a current shunt and from plasmas appearing at pointed electrodes during this time. In negative coronas, such current pulses are frequent [26,29]. The detection of current pulses with a duration of 100-200 ns in positive coronas is reported elsewhere [20].

Our detailed study confirms that corona discharge in a highly inhomogeneous electric field is initiated at a comparatively low voltage which, as expected, increases with increasing the tip radius and diameter of a needle. The start voltages of corona discharge for needles of different sizes and point-plane gaps of different widths are indicated in Table 2.

Table 2. Corona start voltage for different needles

Needle size	Voltage polarity	Gap, cm	Corona start voltage, kV
No. 1b	+	3	6.0
No. 2b	+	3	7.0
No. 2b	+	1	3.8
No. 2b	+	2	4.2
No. 3b	+	3	10.0
No. 3b	-	3	6.5

When going from positive to negative polarity, the start voltage of corona decreases with decreasing the gap width *d* and increases with increasing the tip radius and needle diameter. The data in Table 2 are for needles with

 DOI: https://doi.org/10.30564/jasr.v3i4.2342

spark-blunted tips (index b) and hence with higher corona start voltages compared to sharp ones, all other things being equal.

The initiation of corona at minimal voltages was studied with needle No. 1a having the smallest tip radius (11 μm). When the tip was blunted, the needle was replaced by a fresh one. Such pointed electrodes were needed to produce the highest electric field and to initiate single streamers at low voltages. The power supply was stabilized. Figure 5 shows the start voltage of first streamers versus the gap between needle No. 1a and plane electrode.

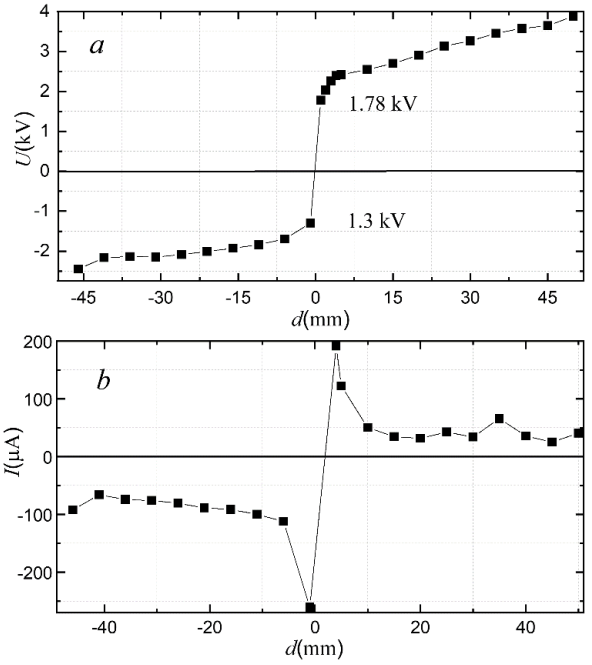

Figure 5. Start voltage of first current pulses (a) and their amplitude (b) versus gap d between needle No. 1a and plane electrode. Negative *d* values are for negative voltage polarity

With sharp needles No.1a, like with blunted ones, the corona start voltage was lower at negative than at positive polarity. Besides, the start voltage of first pulses at positive polarity, compared to negative one, increased faster with d. It should also be noted that although the start voltage of first current pulses increased with d, the current amplitude decreased (Figure 5b). These data are apparently new.

Figure 6 shows the waveforms of first current pulses and pulses in mixed modes at positive and negative voltage polarity for needle No.1b. The time resolution is no worse than 5 ns.

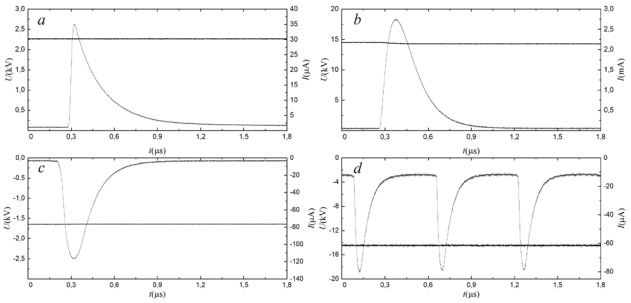

Figure 6. First current pulses (a, c) and pulses in mixed modes (b, d) at different voltages (straight lines) at positive (a, b) and negative polarity (c, d). Gaps 5 (a, c) and 40 mm (b, d). Needle No. 1b

As can be seen, the start voltage of first pulses with *d* = 5 mm is 1.64 kV at negative and 2.26 kV at positive polarity, which agrees with the data of Figure 5a. The waveforms in Figure 6a,c also suggest that at positive polarity, compared to negative polarity, the rise time of the pulse is shorter but its fall time is longer and its width at a level of 0.1 is larger. Increasing the gap to 40 mm increases the start voltage and the amplitude of first current pulses.

It should be noted that the start voltage and the current of coronas depend on not only the tip radius and length of gap but also on the humidity and pressure of air. Our comparative measurements were taken during a short time and under the same weather conditions, and although the parameters did vary from day to day (primarily due to varying air humidity), their tendencies remained unchanged.

The amplitude of pulses and their spacing depended on the voltage and its polarity. At relatively low voltages, the amplitudes of the first corona current pulses are usually larger when a needle electrode is negative. As will be shown below, under these conditions, ball streamers are formed. However, cylindrical streamers are formed from a positive needle with increasing voltage, and the amplitude of the positive corona current pulses increases significantly. For example, at a positive polarity voltage of 8 kV, needle No. 1a, and *d* = 8 mm, they had an amplitude of 6 mA, FWHM of 220 ns, and repetition period of ≥240 μs corresponding to a frequency of ≈4.2 kHz. With the same gap and voltage at negative polarity, they had an amplitude of 56 μA, FWHM of 94 ns, and frequency of 5 MHz, and their steady current component before the next pulse was ≈42 μA. At the same voltage, the pulse repetition frequency for the negative polarity, compared to the positive one, was more than several orders of magnitude higher. As a result, a much higher average corona current was observed at negative polarity. The fact that a train of pulses (Trichel pulses) whose frequency increases with voltage appears in a negative corona after its first pulse is described in many papers. Tables 3 and 4 present data on

DOI: https://doi.org/10.30564/jasr.v3i4.2342

the amplitude of current pulses and their frequency and spacing at different voltages of negative and positive polarity for needle No. 1a with $d = 2$ cm.

Table 3. Amplitude of current pulses, pulse frequency, and pulse spacing in negative coronas from needle No. 1a with $d = 2$ cm

$-U$, kV	I, μA	f, kHz	τ, μs
3.1	5.4-6.4	28.6	35
4.1	6-6.8	30	33.5
5	5.4-6.4	71	14.08
6	5.2-6.8	149	6.73
9.2	5-6.4	281	3.56
10.1	4.2-6.4	345	2.9
12	4.4-5	476	2.1

Table 4. Amplitude of current pulses, pulse frequency, and pulse spacing in positive coronas from needle No. 1a with $d = 2$ cm

$+U$, kV	I, μA	f, kHz	τ, μs
8.8	144	4.49	222.8
9.9	233	5.41	184.7
10.7	389	5.68	176.2
11.4	501	6.17	162.1
12.2	541	7.34	136.3
12.8	689	7.4	135.1
13	809	7.52	133

As noted above, with increasing voltage, cylindrical streamers are formed from a positive needle, and the amplitude of the positive corona current pulses increases significantly.

We think that the recorded current pulses are due to streamers which, as evidenced by discharge images, can be both ball and cylindrical.

3.3 Plasma in Corona Discharges

Our study confirms that in atmospheric pressure air, the start voltage of corona discharge from pointed electrodes measures several kilovolts and that their initiation at any voltage polarity is accompanied by current pulses with a FWHM of 100-200 ns (Figure 6). Because of the low start voltage and amplitude of first corona pulses, the intensity of first streamers is very low and so is the corona intensity near the tip of needles in quasi-steady modes. This makes it difficult to capture the early stage of coronas even with ICCD cameras. Therefore, images of coronas at low voltages (few kilovolts) were taken in the dark at the maximum digital camera sensitivity with long exposure times (mostly, with 15 s). Figure 7 shows the plasma of negative and positive coronas near needle No. 1a.

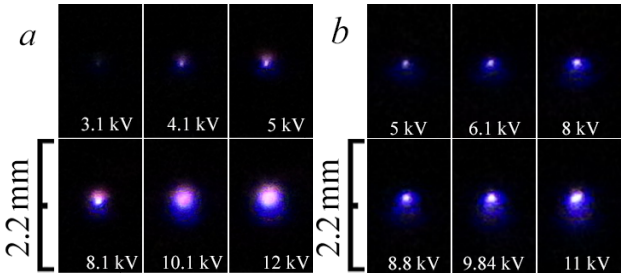

Figure 7. Images of corona discharges near needle No. 1a at negative (a) and positive polarity (b). Length of gap 2 cm. Exposure time 15 s

The size of luminous corona areas depended on the voltage and length of gap. At negative polarity, the corona plasma was ball only in the range of low voltages and was contracted as the voltage was increased, which agrees with data reported elsewhere [4]. At the same voltage, the total emission near the negative needle, compared to the positive one, was higher. At positive polarity, the plasma was ball over a wider voltage range, and as the voltage was increased, jets escaped from the plasma up to the plane electrode (Figure 8a).

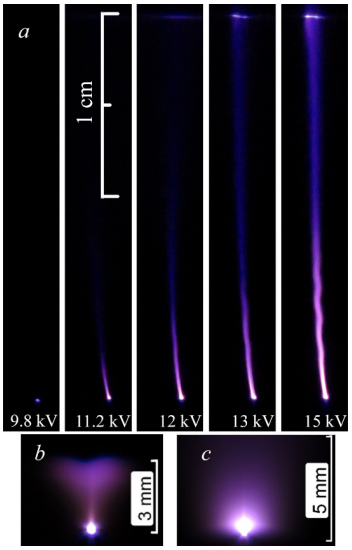

Figure 8. Images of discharges from positive needle No. 2b at $d = 20$ mm (a) and from negative needle No. 1b at $d = 10$ mm, $U = 3.8$ kV (b) and negative needle No. 4 at $d = 10$ mm, $U = 16.9$ kV (c). Exposure time 15 s

The long jets in Figure 8a are cylindrical positive streamers for which the electric field in gap is two-three times smaller than the field for negative streamers [27]. At 15 kV, as can be seen in Figure 8a, such a jet bridges the gap and the corona transforms to a glow discharge which operates stably till the formation of spark channels at high gap voltages. A current-limiting resistor between the

DOI: https://doi.org/10.30564/jasr.v3i4.2342

power supply and needle (Figure 1, R_b) provides the glow discharge stability at atmospheric pressure. The glow-to-spark discharge transition is fast and voltage across the gap decreases significantly. Such a transition at negative polarity can be judged from Figure 3, and glow discharge at negative polarity from Figs. 8*b* and 8*c*, respectively.

Figure 9 shows ICCD images of the plasma of a negative corona near the tip of needle at pulsed voltage.

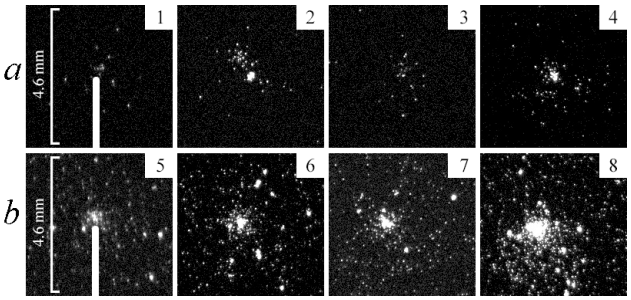

Figure 9. ICCD images of negative coronas near needle No. 1b with d = 9 mm at maximum gap voltages 13 kV (*a*) and 6 kV (*b*). The needle is shown only in frames 1 and 5. Frame duration 200 ns (1, 2, 3), 600 ns (4), 20 μs (5, 6, 7), and 60 μs (8) with no time delay between first (1, 5) and second frames (2, 6) and between second and third (3, 7). Last frames (4, 8) are for coronas within respective first frames (1, 2, 3 and 5, 6, 7)

Because of the low intensity and widely varied start time of first streamers at low voltages with low rates of rise, it was impossible to accurately trace their formation dynamics by ICCD imaging. However, an increase in the emission intensity due to streamers was identified in individual frames ~200 ns long. As can be seen from Figure 9*a*, more intense streamer emission is present in frame 2 and in frame 4 whose duration spans that of frames 1, 2, and 3. Such emission within 200 ns corresponds to the current pulse duration of the first ball streamer (Figure 8*a*, 9.8 kV). Under the conditions considered, the spacing between streamer pulses was much longer than 600 ns, and such images were possible only after tens to hundreds of corona imaging events.

As the frame duration was increased to over 20 μs, the detection of individual streamers failed. The emission intensity was determined by the quasi-steady corona current and was the same at the same frame durations. Our experiments on the detection of first streamers at a pulse voltage rise time of 500 ns confirmed the results reported elsewhere [20]. Increasing the gap voltage at the rise of first streamers allowed us to capture their emission at negative polarity in frames 200 ns and 100 ns long, which roughly corresponds to the current FWHM through the gap. However, their formation dynamics at such frame durations was untraceable. We think that it is similar to what is observed at voltage pulses of tens of nanoseconds [32]. With a frame duration of ~10 ns and shorter, the emission intensity of negative streamer was insufficient for its identification, though the total emission intensity at the negative needle, compared to the positive one, was higher due to higher streamer formation rates (Figure 7).

At positive voltage polarity with the same pulse amplitude, we could clarify some details of the formation dynamics of individual streamers. For example, at high voltages, a streamer head moving off the tip was detected in frames of 10 ns. This suggests that increasing the voltage increases the emission intensity of single positive streamers compared to negative ones, which correlates with current pulse amplitudes. In Figure 6*a, b*, the current pulse amplitudes at different polarities are about equal, and in Tables 3, 4, they are much higher at positive polarity. Such a mode is observed during the formation of cylindrical positive streamers (Figure 8*a*) from the plasma created at the needle tip by a ball streamer (Figure 7*b*). Figure 10 shows ICCD images of a cylindrical positive streamer at a constant gap voltage.

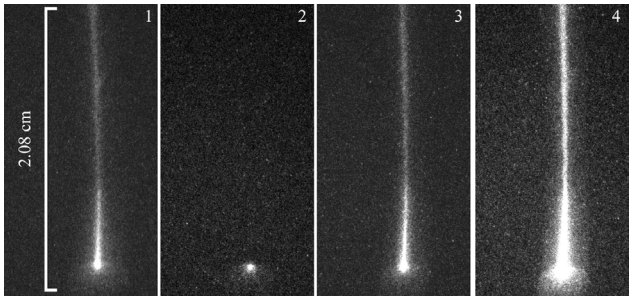

Figure 10. ICCD images of cylindrical positive streamer from needle No. 1b with d = 21 mm at maximum gap voltage 17.3 kV. Frame durations 100 μs (1, 2, 3) and 300 μs (4) with no time delay between first (1) and second frame (2) and between second and third (3). Last frame (4) is for discharge within first three frames.

As can be seen in Figure 10, such a streamer is captured in frames 1 and 3 due to their large spacing, and in frame 4, two cylindrical streamers are overlapped. With no cylindrical streamer in frame 2, only the region near the tip is luminous at a quasi-steady corona current. Such a bright spherical region with cylindrical streamers is also clearly visible in Figure 8*a*.

4. Discussion

Initiation of ball and Cylindrical Streamers

Our study of corona discharges in atmospheric pressure air evidence that (1) both negative and positive coronas develop via the ball streamers near the needle tip at several kilovolts and that (2) positive ball streamers start at

DOI: https://doi.org/10.30564/jasr.v3i4.2342

higher voltages and positive cylindrical streamers at lower voltages compared to negative ones.

As already noted, the electric field needed for a negative streamer is two-three times higher than that for a positive one [27]. However, in our study, like in others, negative coronas at low voltages were initiated and cylindrical streamers in low electric fields were detected, suggesting two types of corona streamers: ball in high electric fields and cylindrical in more low electric fields. We think that it is the high electric field at needle tips, which provides the initiation of ball streamers.

Figure 11 shows the distribution of electric field strength for needles No. 1a and No. 1b at 2 kV and $d = 40$ mm.

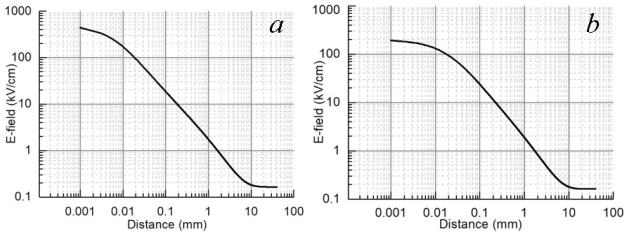

Figure 11. Electric field strength versus distance from needles No. 1a (a) and No 1b (b) at 2 kV, $d = 40$ mm

From Figure 11 it follows that the electric field strength at the tip of needle No. 1a at 2 kV is higher than 0.4 MV/cm. This value is of the order of the electric field at pointed electrodes in nanosecond pulsed diffuse discharges formed by wide (ball) streamers [28,31,32]. Hence, similar mechanisms can be expected for discharges from sharp points at rates of voltage rise of $<10^6$ V/s and $>10^{12}$ V/s. The rates $>10^{12}$ V/s correspond to diffuse discharges involving fast and runaway electrons at negative voltage polarity [33] and X rays at positive polarity [34].

Although the electric field for coronas from thin needles is several times lower than the field for nanosecond discharges with pulse amplitudes of tens to hundreds of kilovolts, the time during which their tips is kept at high voltage is much longer. This causes charge accumulation at needle tips, avalanche growth to critical sizes, and ball streamer formation at both voltage polarities.

The emission of electrons from negative tips is more efficient than their emission from positive ones. Besides, nanoparticles [35] and dielectric films, including carbon [36], lower the field emission threshold. Therefore, the start voltage of negative coronas is lower.

Under certain conditions, the appearance of primary electrons in length of gaps can be associated with natural background ionizing radiation, which gives ~10^3 electron/cm^3 in 1 ns [27], and with dark current, which is recorded at high instrument sensitivity. However, these contributions are likely important only at positive voltage polarity. With positive needle tips, higher voltages are needed to make the ion concentration sufficient for the start of a positive streamer, suggesting that the generation of primary electrons, in this case, is less efficient. Nevertheless, ball streamers do arise at positive polarity. The motion of ball streamers stops because the electric field decreases rapidly with distance from pointed electrodes and its average value in corona discharges is comparatively small. Under such conditions, the flow of quasi-steady current is provided by charged particle drift in the region of low electric fields and by photoemission via shortwave emission from the plasma that remains as a dense cloud at the tip of a pointed electrode due to its high electric field and ongoing air ionization there. As the voltage of positive polarity at the tip is increased, classical cylindrical streamers start escaping from the plasma cloud, as evidenced by our ICCD imaging. The electric field for the start of cylindrical cathode streamers is much lower and their length is larger than those of negative streamers in corona discharges are.

When cylindrical streamers develop (Figs. 8 and 10), the pulsed current increases greatly (Table 4) due to dynamic displacement current [28,37]. As a cylindrical streamer moves from a pointed to a plane electrode kept in a low electric field, capacitive charging occurs between its front and plane electrode. As the voltage is increased, such streamers reach the plane electrode, forming a glow discharge which is further transformed to a spark. Because of the cylindrical streamer formation, the breakdown voltage is lower at positive than at negative voltage polarity.

The current recorded during the formation of ball streamers is also contributed by dynamic displacement current. However, its amplitudes in corona discharges (due to small streamer sizes) are lower than its amplitudes in nanosecond diffuse discharges [28,37-40]. Measurement data on electric fields at ionization wave fronts during breakdowns are reported elsewhere [41-43].

5. Conclusion

Our research confirms that both negative and positive coronas in atmospheric pressure air develop via ball streamers which appear in the vicinity of electrodes with a small radius of curvature (~10 μm). As it follows from calculations, the electric field at the tip of a needle reaches several hundred kilovolts per centimeter at a voltage of a few kilovolts. These conditions approximate those for the generation of fast electrons and X-ray quanta in diffuse discharges [33].

The start voltage of positive streamers, compared to negative ones, is higher due to low initial electron concentrations in air. The lower start voltage of negative stream-

 DOI: https://doi.org/10.30564/jasr.v3i4.2342

ers is due to more efficient electron emission from metal cathodes. The presence of positive ball streamers suggests that the plasma created at positive needle tips emits short-wave photons, which provide their initiation in a high electric field through air preionization.

At the same voltage, the average current of negative corona with ball streamers are higher and their luminous region is larger than those of positive ones, which can be explained by more efficient electron emission from pointed cathodes and by higher frequencies of Trichel pulses. Their frequency at negative polarity, compared to positive, is more than two orders of magnitude greater.

The average electric field strength for the start of positive cylindrical streamers is two-three times lower than its value for negative ones. When cylindrical streamers start from positive needle tips, the amplitude of current pulses increases greatly, going above their amplitude at negative polarity with the same voltage level. However, in the same conditions, the average current of positive coronas is lower than that of negative ones.

From our study it follows that the ignition of coronas from pointed electrodes of any form and polarity begins with ball streamers due to electric field amplification and that, the initiation of a breakdown at positive polarity is due to cylindrical streamers developing from a plasma cloud near near a needle.

Increasing the voltage causes successive discharge transitions from mode to mode. At negative voltage polarity, first comes a dark discharge, and then, a corona with a ball streamer, a corona with steady and pulsed currents, a glow discharge, and a spark. At positive voltage polarity, the sequence of modes includes a dark discharge, a corona with a ball streamer, a quasi-steady corona with rare pulses, a corona with cylindrical streamers, a glow discharge, and a spark. The transition to a glow discharge only little affects the current—voltage characteristic, whereas the transition to a spark involves a steep decrease in the gap voltage and a considerable increase in the amplitude of current pulses.

Acknowledgments

This work was carried out as part of the project of the Russian Science Foundation no. 18-19-00184.

References

[1] L. Léger, E. Moreau, G. G. Touchard. IEEE T. Ind. Appl. 2002, 38(6): 1478.

[2] M. Simek, M. Clupek. J. Phys. D: Appl. Phys. 2002, 35(11): 1171.

[3] Y. S. Akishev, G. I. Aponin, M. E. Grushin, V. B. Karal'nik, M. V. Pan'kin, A. V. Petryakov, N. I. Trushkin. Plasma Phys. Rep. 2008, 34(4): 312.

[4] S. B. Afanas'ev, D. S. Lavrenyuk, I. N. Petrushenko, Y. K. Stishkov. Tech. Phys. 2008, 53(7): 848.

[5] D. Z. Pai, D. A. Lacoste, C. O. Laux, Jour. Appl. Phys. 2010, 107(9): 093303.

[6] M. Sabo, J. Páleník, M. Kučera, H. Han, H. Wang, Y. Chu, Š. Matejčík, Int. J. Mass Spectrom. 2010, 293(1-3): 23.

[7] T. Shao, V. F. Tarasenko, C. Zhang, D. V. Rybka, I. D. Kostyrya, A. V. Kozyrev, P. Yan, V. Y. Kozhevnikov, New J. Phys. 2011, 13(11): 113035.

[8] L. Liu, Z. Zhang, Z. Peng, J. Ouyang, J. Phys. Conf. Ser. 2013, 418(1): 012092.

[9] Y. Zheng, B. Zhang, J. He. Phys. Plasmas, 2015, 22(2): 023501.

[10] X. Li, X. Cui, T. Lu, Y. Liu, D. Zhang, Z. Wang. IEEE Trans Dielectr Electr Insul. 2015, 22(2): 1314.

[11] A. El-Tayeb, A. H. El-Shazly, M. F. Elkady, A. B. Abdel-Rahman. Plasma Phys. Rep. 2016, 42(9): 887.

[12] X. Zhu, L. Zhang, Y. Huang, J. Wang, Z. Liu, K. Yan. Plasma Sci. Technol. 2017, 19(7): 075403.

[13] V. F. Tarasenko, E. K. Baksht, E. A. Sosnin, A. G. Burachenko, V. A. Panarin, V. S. Skakun. Plasma Phys. Rep. 2018, 44(5): 520.

[14] Y. Guan, R. S. Vaddi, A. Aliseda, I. Novosselov. Phys. Plasmas, 2018, 25(8): 083507.

[15] Y. K. Stishkov, A. V. Samusenko, I. A. Ashikhmin. Phys.-Uspekhi, 2018, 61(12): 1213.

[16] R. Bálek and S. Pekárek, Plasma Sources Sci. T. 2018, 27(7): 075019.

[17] Q. Gao, X. Wang, A. Yang, C. Niu, M. Rong, L. Jiao, Q. Ma. Phys. Plasmas, 2019, 26(3): 033508.

[18] B. B. Baldanov, A. P. Semenov, T. V. Ranzhurov, Bull. Russ. Acad. Sci.: Phys. 2019, 83(11): 1366.

[19] Y. Guo, S. Li, Z. Wu, K. Zhu, Y. Han, N. Wang. Phys. Plasmas, 2019, 26(7): 073511.

[20] V. F. Tarasenko, V. S. Kuznetsov, V. A. Panarin, V. S. Skakun, E. A. Sosnin, E. K. Baksht. JETP Letters, 2019, 110(1): 85.

[21] N. G. C. Ferreira, D. F. N. Santos, P. G. C. Almeida, G. V. Naidis, M. S. Benilov, J. Phys. D: Appl. Phys. 2019, 52(35): 355206.

[22] W. Liu, Q. Zheng, M. Hu, L. Zhao, Z. Li. Plasma Sci. Technol. 2019, 21(12): 125404.

[23] Y. Cui, C. Zhuang, R. Zeng, Appl. Phys. Lett., 2019, 115(24): 244101.

[24] M. Cernak, T. Hoder, Z. Bonaventura. Plasma Sources Science and Technology. 2020, 29(1): 013001 .

[25] L. Li, J. Li, Z. Zhao, C. Li. Phys. Plasmas, 2020, 27(2): 023508.

[26] L. B. Loeb. Electrical coronas, their basic physical mechanisms, Univ of California Press, 1965.

DOI: https://doi.org/10.30564/jasr.v3i4.2342

[27] Yu. P. Raizer. Gas Discharge Physics, Berlin: Springer, 1997.
[28] D. V. Beloplotov, M. I. Lomaev, D. A. Sorokin, V. F. Tarasenko. Phys. Plasmas, 2018, 25(8): 083511.
[29] G. W. Trichel. Phys. Rev. 1938, 54: 1078.
[30] V. S. Kuznetsov, V. F. Tarasenko, E. A. Sosnin. Russ. Phys. J. 2019, 62(5): 893.
[31] G. V. Naidis, V. F. Tarasenko, N. Y. Babaeva, M. I. Lomaev, Plasma Sources Sci. Technol. 2018, 27(1): 013001.
[32] V. F. Tarasenko, G. V. Naidis, D. V. Beloplotov, I. D. Kostyrya, N. Yu. Babaeva. Plasma Phys. Rep. 2018, 44(8): 746.
[33] V. F. Tarasenko. Plasma Sources Sci. Technol. 2020, 29(3): 034001.
[34] C. V. Nguyen, A. P. J. Van Deursen, E. J. M. Van Heesch, G. J. J. Winands, A. J. M. Pemen. J. Phys. D: Appl. Phys. 2009, 43(2): 025202.
[35] E. Kalered, N. Brenning, I. Pilch, L. Caillault, T. Minéa, L. Ojamäe, Phys. Plasmas, 2017, 24(1): 013702.
[36] A. Andronov, E. Budylina, P. Shkitun, P. Gabdullin, N. Gnuchev, O. Kvashenkina, A. Arkhipov. Journal of Vacuum Science & Technology B, Nanotechnology and Microelectronics: Materials, Processing, Measurement, and Phenomena, 2018, 36(2): 02C108.
[37] T. Shao, V. F. Tarasenko, C. Zhang, A. G. Burachenko, D. V. Rybka, I. D. Kostyrya, M. I. Lomaev, E. Kh. Baksht, P. Yan. Rev. Sci. Instrum. 2013, 84(5): 053506.
[38] S. Chen, L. C. J. Heijmans, R. Zeng, S. Nijdam, U. Ebert. J. Phys. D: Appl. Phys. 2015, 48(17): 175201.
[39] D. V. Beloplotov, V. F. Tarasenko, D. A. Sorokin, M. I. Lomaev. JETP Lett., 2017, 106(10): 653.
[40] D. A. Sorokin, V. F. Tarasenko, D. V. Beloplotov, M. I. Lomaev. J. Appl. Phys. 2019, 125(14): 143301.
[41] J. J. Lowke, F. D'Alessandro. Journal of Physics D: Applied Physics, 2003, 36(21): 2673.
[42] E. M. Van Veldhuizen, and W. R. Rutgers. J. Phys. D: Appl. Phys. 2003, 36(21): 2692.
[43] E. Wagenaars, M. D. Bowden, G. M. W. Kroesen. Physical review letters, 2007, 98(7): 075002.

 DOI: https://doi.org/10.30564/jasr.v3i4.2342

BILINGUAL PUBLISHING CO.
Pioneer of Global Academics Since 1984

Journal of Atmospheric Science Research
https://ojs.bilpublishing.com/index.php/jasr

ARTICLE

Climatic Changes and Their Effect on Wildlife of District Dir Lower, Khyber Pakhtunkhwa, Pakistan

Asad Ullah[1] Sayyed Iftekhar Ahmad[1] Rafi Ullah[2] Atta Ullah Khan[3] Sikandar Khan[4] Waheed Ullah[5] Abdul Waris[6*]

1. Department of Environmental Sciences, Government Degree College Gulabad Chakdara, Dir Lower, Pakistan
2. Plant Ecology and Dendroecology Labartory, Department of Botany, University of Malakand, Pakistan
3. Department of Biotechnology, University of Malakand Chakdara, Dir Lower, Pakistan
4. Pakistan forest Institute, University of Peshawar, Pakistan
5. Department of Environmental Science, COMSATS University Islamabad, Abbotabad Campus, Pakistan
6. Department of Biotechnology, Quaid-i-Azam University Islamabad, Pakistan

ARTICLE INFO

Article history
Received: 12 August 2020
Accepted: 11 September 2020
Published Online: 30 September 2020

Keywords:
Climate change
Wildlife
Temperature
Rainfall
Lower Dir
Pakistan

ABSTRACT

Climatic changes and their impact are increasingly evident in Pakistan, especially in the mountainous regions. Mountain ecosystems are considered to be sensitive indicators of global warming; even slight variations in temperature can lead to significant shifts in local climate, which can, in turn, drastically affect the natural environment, subsequently altering people's lifestyle and wildlife habitats. The targeted area for the present research was Lower Dir District, Pakistan. The study gathered the required information from primary and secondary sources. Secondary data on temperature and precipitation were obtained from various sources, i.e., local CBO, including WWF Pakistan. Based on information gathered on climate change and wildlife, a detailed questionnaire was designed. Results showed that no regular pattern of the increase was found in temperature from 2010 to 2018; the same was noticed in the rainfall decrease pattern. Results also showed that the leading causes behind climatic changes are an increase in greenhouse gases due to pollution by industries, vehicles, crushing plants, deforestation, and some natural phenomena such as floods. The study showed that more than 80% of the respondents agreed that climatic effects have a significant impact on wildlife, i.e., the existence of wildlife falls in danger due to climatic changes as it may lead to habitat change, making it difficult for the survival and adaptation of the wildlife. Hence, in consequence, it leads to migration, low growth rate, an increase in morbidity and mortality rate, and finally leading to the extinction of the species or population. It is concluded from the study that people are severely noticing the climatic change and its leading causes are greenhouse gases and deforestation. To control climatic changes and wildlife extinction, we need an appropriate policy for forest conservation, wildlife conservation, prevent hunting, industrial pollution control, vehicle pollution control, increase in plantation, awareness of policy for the control of climatic changes, etc.

**Corresponding Author:*
Abdul Waris,
Department of Biotechnology, Quaid-i-Azam University Islamabad, Pakistan;
Email: awaris@bs.qau.edu.pk

DOI: https://doi.org/10.30564/jasr.v3i4.2275

1. Introduction

Climate is a long-term weather pattern that describes a region [1,2]. Climate change is a universal threat to many sectors, such as food production, water and energy, agriculture, human health, economy, and biodiversity [3]. Climate changes and its impacts are increasingly evident in Pakistan, especially in the mountainous regions. Mountain ecosystems are considered the sensitive indicators of global warming; even a slight increase or decrease in temperature can cause significant shifts in the local climate, which can, in turn, drastically affect the natural environment and subsequently, humans and wildlife [4]. There are many causes of climate change like greenhouses gases, deforestation, industrialization, urbanization, etc. which may lead to global warming, glaciers melting, disasters, floods, migration of birds and wild animals, wildlife and other species extinction [5]. Climate changes could occur naturally as a result of the change in the sun's energy or Earth's orbital cycle (natural climate forcing), or it could occur as a result of persistent anthropogenic forcing; such as the addition of greenhouse gases, sulfate aerosols, black carbon to the atmosphere and through land-use change [6,20]. The Earth's global surface temperature has risen by approximately 0.8 °C while in the 70s by 0.5 °C. This increase in temperature is directly proportional to the increase of atmospheric concentration in greenhouse gases, mainly methane and carbon dioxide, for which human emissions are considered the primary cause. The majority of scientists believe that a further increase in greenhouse gas emissions could threaten humanity [4].

Climate changes will have severe effects on the health of humans, domestic animals, and wildlife. Climate change is not only affecting the large organisms, but it also has a detrimental effect on micro-habitat [25]. In the lowland forests in Costa Rica, the reptilian and amphibian populations have declined via climate change on the humid leaf litter micro-habitat of the forest floor [5]. Fewer sightings of wildlife – bird diversity dropped and Black Bear, wolf, snow Leopards, Markhor, and Himalayan Ibex, no longer seen in northern Pakistan [6].

Greenhouse gases like carbon dioxide absorb heat emitted from the earth. The increase of these gases in the atmosphere leads to warm earth by trapping more and more heat. Human activities like the burning of woods and fossil fuels lead to the formation of gases that contributes to a greenhouse, air pollution, and increasing atmospheric carbon dioxide up to 40%, with more in half the increase occurring since the 1970s. Since 1900 the global temperature has been raised by 0.8°C (1.4°F) [24]. Most of the studies showed an increase in temperature is due to an increase in the release of CO2 and other gases that contribute to the greenhouse. Further increase in these gases will cause further climate change, including a substantial increase in regional climate changes and global average surface temperature. Over many decades, a long time depends only on the amount of greenhouses gases (CO2) emitted as a result of human activities [12].

There is a specific range of environmental conditions for every organism to live. If some abiotic factors such as oxygen concentration shift or precipitation or temperature increase or decrease in such a way that these are outside the range required for a particular specie, then in that habitat, the existence of particular species becomes impossible [13]. Variations in global temperatures have wide-ranging effects on environmental conditions and are expected to decline the population of species ranging from tropical corals to Midwestern mammals [14]. Many scientists believe that global temperature increases due to human activities like the burning of fossil fuels and woods. While some dispute this claim, arguing that temperature increases are part of the earth's natural climate cycle [15]. Some events can eliminate a particular species, such as a massive volcanic eruption, an asteroid strike, or even a rapid loss of large areas of critical and unique habitat because of deforestation. To date, evidence suggests that deforestation is currently and is projected to continue to be the leading indirect and direct cause of reported extirpations [16]. For example, because of the ongoing and past deforestation, it is predicted that approximately 21% of the Southeast Asian forest species will be lost by 2100 [17]. The ecosystem and biological community changes precipitated by invasive species represent another leading cause of biodiversity loss [18]. Climate change mediated by humans represents a potentially disastrous sleeping giant in terms of future biodiversity losses [19]. There are five principal ways through which the species can be affected by climate warming. These are Range shifts, either pole-ward or upward in elevation; alterations of species densities (including altered community composition and structure); Changes in morphology, such as body size; behavioral changes, such as the phenology (seasonal timing of life cycle events) of migration, breeding, and flowering; and Reduction in genetic diversity that leads to inbreeding depression [7].

This study has been conducted in congruence with other research works being conducted. This means that the study highlights the areas which are not entirely addressed by the existing studies. Thus, it serves as an ancillary tool to support the ongoing studies on biodiversity, glaciers, wildlife, and forestry, all directly affected by climate change patterns.

 DOI: https://doi.org/10.30564/jasr.v3i4.2275

2. Materials and Methods

The details of the study area are described below.

2.1 Targeted Area and Duration

The study area that we targeted were the District: Dir Lower, KP, Pakistan. The field study for the case of study was conducted from 10 June-10 November 2018.

2.2 Methodological and Structure Approach

Research Design, Research Instrument, and Research Phases and Activities

The present study was collected the required information from primary as well as from secondary sources. Primary field data was collected through documenting observations of local communities. A survey questionnaire was designed to gather primary data for the study. The study process was involved in several steps, including:

2.3 Secondary Data

Secondary data on temperature and precipitation were obtained from various sources, the local CBO (Community Based Organization), including WWF (World Wide Fund) Pakistan. Other internet-based research and literature helped in identifying the leading climate change concerns specific to areas.

2.4 Questionnaire

Based on information collected on climate change and wildlife, a questionnaire was designed. The questionnaire included information on climate change and its impact on wildlife and wildlife affected by climate change.

Pre-testing

The approved questionnaire was pre-tested in a village called Hoppy. Based on the interview conducted, minor revisions were made in the questionnaire to concise and incorporate contextual evidence and make the tool more focused (on climate change-related indicators), so that utility and the targeted response were ensured.

2.5 Field Visit Plan

The field visit schedule encompassed the following components. Targeted areas and villages were covered by each of the two survey teams sample size. For the survey, the total number of household members (male and female) were interviewed. Each made the date of visits to the two survey teams.

2.5.1 Data Collection

Project partners conducted the field of the survey; data were collected from the interviewees. In addition to interview sessions with general community members, local key persons were also interviewed.

2.5.2 Database Development

A specific format was designed to feed in the field data collected. The entire information gather was consolidated and stored electronically.

2.5.3 Data Analysis

The data analysis procedure involved preliminary coding and sorting of data, mostly through data reduction (write-ups of field notes) and data reconstruction (development of categories, findings, conclusions, connections to existing literature, integration of concepts). The data was then presented in a narrative report of findings with descriptive and interpretative details.

3. Results

3.1 The Rate of Monthly Rain

As a global temperature change, the rain rate in DIR Lower changes, as shown in the graph No.1 (Pakistan Meteorological Department). On Jan and Feb 2010-2018, there is a sharp increase up to 250mm except found in 2010 and 2018. And then a sharp decrease of 50 mm in April and May in 2010, 2011, 2013, 2014, 2015, 2016, 2017, and 2018, respectively. In June and August, a sharp increase of 100mm-200mm was found 2010- 2015 except 2011. In September and October, the rain rate was found mostly below 50 mm expect 2014. There was a sharp increase up to above 150 mm. In November and December, there was a mostly linear rate below 50 mm. The graph shows two regular sharp increases in January and July and a regular sharp decrease in May and September, while mostly the increase and decrease in the raining rate is not regular, especially and March, April, June, and October, as shown in Table 1 and Figure 1.

Table 1. Monthly total rain rate (mm) of the past eight years (2010-2018)

YEAR	JAN	FEB	MAR	APR	MAY	JUN	JUL	AUG	SEP	OCT	NOV	DEC
2010	62	220	44	31	40.5	28	424	153	56.6	0	0	0
2011	25	258	88	72	21	40	54	61	33	66	15	0
2012	82	94	35	89	39	3	74	150	107	14	20	69
2013	6	247	103	97	22	98	97	205	55.2	30	52	0
2014	0	148	175	158	50	50	36.2	50	68	163	23	0
2015	117.0	241.0	252.0	183.0	102.0	98.0	175.0	146.0	35.0	103.0	182.0	63.0
2016	114.5	101.0	323.0	236.0	88.0	73.0	114.0	176.0	43.0	8.0	9.0	29.0
2017	290.0	190.0	91.0	114.0	65.0	86.0	62.0	106.0	97.0	40.0	26.0	44.0
2018	0.0	73.0	77.0	85.0	71.0	31.0	110.0	82.0	23.0	35.0	35.0	21.0

DOI: https://doi.org/10.30564/jasr.v3i4.2275

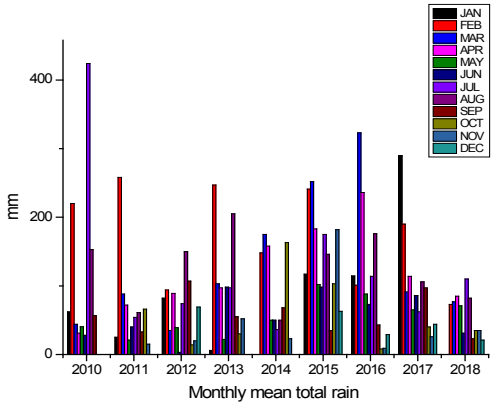

Figure 1. Monthly total rain rate (mm) of past eight years (2010-2018)

3.2 Monthly Mean Minimum Temperature

The data were collected from the Pakistan Meteorological Department, which shows variation clearly in minimum temperature as the year past. While 2010 seems warm as compared to the next three years (2011, 2012, and 2013), while the next two years (2014-2018) is warm more than the past two years (2012 and 2013). Thus a little increase is found overall in the last five years. The average minimum temperature in the last five years was 13.0°C. The lowest temperature was found in 2011 -1.3°C followed by -1.5 in December 2010, as shown in Table 2 and Figure 2.

Table 2. Monthly mean Minimum temperature of the past eight years (2010-2018)

YEAR	JAN	FEB	MAR	APR	MAY	JUN	JUL	AUG	SEP	OCT	NOV	DEC
2010	1.8	5.3	12.5	16.7	20.5	22.8	24.4	23.7	19	14.7	5.4	-1.5
2011	-1.7	3.3	9	12.4	19.7	23.4	23	22.8	18.7	12.4	7.5	-1.3
2012	0	2.1	8.5	13.6	16.5	21.9	24	22.3	17.6	11.6	6.3	3.6
2013	1.2	3.8	8.5	13.9	19.7	24.1	23.7	22.8	19.9	15.6	5.6	2.3
2014	0.8	4.7	8.3	13.6	17.7	23	24.6	22.6	20.1	14.7	6	0.5
2015	1.5	5.3	9.1	14.1	19.3	22.5	24.1	22.8	0	14.4	7.6	2.3
2016	-2.6	-1.9	3.0	6.1	11.0	14.5	17.3	14.4	12.3	6.4	2.1	-0.9
2017	-2.6	-1.2	2.6	6.8	10.7	14.2	18.2	15.7	11.2	5.7	0.9	-2.2
2018	0.2	4.4	10.9	15.1	19.9	24.0	24.3	24.0	20.0	13.1	7.0	0.3

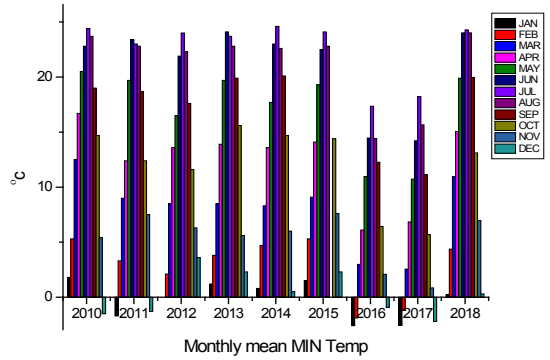

Figure 2. Monthly mean Minimum temperature of the past eight years (2010-2018)

3.3 Monthly Mean Maximum Temperature

The data were collected from the Pakistan Meteorological Department, which shows variation clearly in maximum temperature as the year past. 2010 was the warmest year in the past five years. The next year 2011, was also warmer while the little variation was found in 2012 and 2103, mostly in January and February, while 2014 is the second warmest year in the last five years followed by 2015 to 2018. The overall values show a little increase in the last five years. The highest temperature was found in July in 2014, 39.6 °C, followed by 39.0°C in June 2011 and July 2012, as shown in Table 3 and Figure 3.

Table 3. Monthly mean maximum temperature of the past eight years (2010-2018)

YEAR	JAN	FEB	MAR	APR	MAY	JUN	JUL	AUG	SEP	OCT	NOV	DEC
2010	18.7	15.5	27.2	31.7	34.5	37.3	36.4	33.1	32.9	30.3	23.6	16.5
2011	16.3	14.1	23.9	27.9	37.7	39	36.3	35.6	33.4	27.7	22.1	16.9
2012	13.3	14.1	22	28	33.4	38.9	39	35.9	32.8	29.4	22.7	15.4
2013	15.5	16.3	23.2	28.6	36.3	38.4	36.4	34.9	33.7	30	20.9	17.7
2014	17.2	16.8	19.5	27.2	32.8	39.6	38.1	36.8	34.8	28.3	21.4	17.7
2015	15.6	17.6	21.4	28.7	34.2	36.9	35.7	35	0	29.4	20	16.4
2016	14.6	17.7	18.4	22.7	30.4	33.3	32.9	31.9	31.2	28.5	22.8	20.1
2017	10.1	15.4	18.7	25.3	30.5	32.5	32.4	32.1	30.7	28.0	21.7	17.4
2018	17.7	19.2	25.6	30.2	33.3	39.8	36.8	35.9	35.2	29.3	22.1	17.3

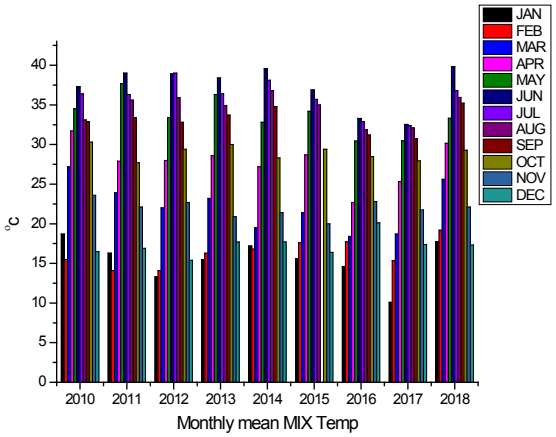

Figure 3. Monthly mean maximum temperature of the past eight years (2010-2018)

4. Discussion

Results show a notable change found in Temperature, rainfall rate, snowfall, drought, deforestation, and indirect effect on climate. Also, the effect of climatic change has been observed, and the most notable effect is on wildlife and human health

4.1 Changes in Climate

We observed that many factors harm climate through

 DOI: https://doi.org/10.30564/jasr.v3i4.2275

results analysis, and these factors are dominating day by day. Most people observe climate change, and human activities with natural phenomena enhance these factors' effects. As our result showed that temperature somewhat changes and high variation is found in the past eight years, many other surveys like The study of Farooqi, Khan [8] showed that Analysis of the past depicts that our climate is changing. The main factors involved are greenhouse gas emissions, natural phenomena, etc. and their effect on water resources, and subsequently affect food supply, health, industry, transportation, and ecosystem sustainability. Our study also mentions that the major causes of climatic change are deforestation; mostly, 100% responders were agreed. It is a significant factor contributing to climate change in this area, which is in line with the previous study of Malmsheimer Bowyer [9]. Our study showed that rapid deforestation also has a significant contribution to a decrease in rainfall and an increase in greenhouse gases and subsequently causes climatic change, the same wise the previous study of da Silva Dias [10] showed the same effect. According to the current study, the incidence of diseases has a prominent effect on the wildlife growth rate caused by polluted water caused by deforestation, flooding, industrialization, urbanization, sewage, etc. The same results were obtained by the study of Malmsheimer, Bowyer [9].

4.2 Effect of Climatic Change on Wild Life

As the results showed, dramatic changes occur in the climate, which leads to severe problems such as Wildlife extinction, health problems, a decrease in crop production, a decrease in drink water, and many more. The climatic changes cause the rapid habitat loss of wildlife and pollution, which forces them to displace or eliminate or extinct. When an environment altered abruptly or systematically at a rate above the average background change, or beyond the capacity of adaptation via natural selection, specialist species with narrow ecological niches often bear the brunt of progressively unfavorable conditions such the loss of habitat and degradation (studied by Sodhi, Lee) [7].

A study of the US Department of the interior, fishes, and wildlife Manchester showed that One-third of 165 species of wetland breeding birds show medium or high vulnerability to climate change, and black ducks have been identified as the most susceptible to sea-level rise associated with a warming climate [22].

Our study mention all the threats toward wildlife, primarily through climate change while the same case was Studied by Kronstadt [11], showed that the moderate climatic change puts some of this biodiversity at considerable risk, the rise in average global temperature will influence the length and severity of season and the frequency and severity of floods and drought, increasing the prevalence of fire and predisposition to pests and pathogens with the expected impact on forest habitats and species. About one quarter of vascular plants and higher animals on the globe are estimated to be at increasingly high risk of extinction as temperature rise by 2- 3C above pre-industrial levels. Even more modest losses in biodiversity would likely affect the ecosystem services [23].

As the global average temperature continues to rise, it is essential to develop strategies to conserve species and habitats that are unable to adapt, measure to reduce the impact of other human pressure, which still exceed those of climate change in most case are also likely to help reduce the overall vulnerability of forest ecosystem to climate change, more radical measure for adopting forests and wildlife to climate change include modifying or newly creating habitats, trans-locating whole animal and plant communities and moving boundaries of the protected area.

5. Conclusion

It is concluded from the study that people are severely noticing the climatic change and their leading causes were greenhouse gases and deforestation. So, it is vital to decrease those activities whose is responsible for greenhouses gases and also to decrease deforestation and promote forestation locally as well as globally. The study also concluded that industrialization and vehicles are responsible for the greenhouse gases that cause global warming in consequences their effect on the environment are, decrease in rain rate, increase in diseases, migration of birds, decrease in drink water for human and wildlife. As the climatic changes increase, wildlife's life becomes in danger and leads to migration or extinction. To control the climatic change and wildlife extinction, we need a forest conservation policy, wildlife conservation, prevent hunting, industrial pollution control, vehicle pollution control, increase in plantation, awareness of the policy for the control of climatic change, etc.

References

[1] Change, I.C. IPCC third assessment report. World Meteorological Organisation and UNEP http://www.ipcc, 2001.

[2] Joos, F., et al. Global warming feedbacks on terrestrial carbon uptake under the Intergovernmental Panel on Climate Change (IPCC) emission scenarios. Global Biogeochemical Cycles, 2001, 15(4): 891-907.

[3] McMichael AJ, Powles JW, Butler CD, Uauy R.

DOI: https://doi.org/10.30564/jasr.v3i4.2275

Food, livestock production, energy, climate change, and health. The lancet, 2007, 370(9594): 1253-63.
[4] Rockström, J., et al. A safe operating space for humanity. nature, 2009, 461(7263): 472-475.
[5] Hasnat GT, Kabir MA, Hossain MA. Major environmental issues and problems of South Asia, Particularly Bangladesh. Handbook of environmental materials management. 2018: 1-40.
[6] Bazargan, A., A multidisciplinary introduction to desalination. Stylus Publishing, LLC, 2018.
[7] Sodhi, N.S., et al. A meta□analysis of the impact of anthropogenic forest disturbance on Southeast Asia's biotas. Biotropica, 2009, 41(1): 103-109.
[8] Farooqi, A.B., A.H. Khan, H. Mir. Climate change perspective in Pakistan. Pakistan Journal of Meteorology, 2005, 2(3).
[9] Malmsheimer, R.W., et al. Managing forests because carbon matters: integrating energy, products, and land management policy. Journal of Forestry. 2011, 109(7S): S7-S50.
[10] da Silva Dias, M.A.F. Forest and Rainfall Interactions in the Amazon Basin. 2008.
[11] Kronstadt, K.A. Flooding in Pakistan: Overview and issues for congress. 2010: DIANE Publishing.
[12] Solomon S, Plattner GK, Knutti R, Friedlingstein P. Irreversible climate change due to carbon dioxide emissions. Proceedings of the national academy of sciences. 2009, 106(6): 1704-9.
[13] Sodhi NS, Brook BW, Bradshaw CJA. Causes and consequences of species extinctions. In: Levin SA, editor. The Princeton Guide to Ecology. Princeton, NJ:Princeton University Press: 2009: 514-20.
[14] Handmer J, Honda Y, Kundzewicz ZW, Arnell N, Benito G, Hatfield J, Mohamed IF, Peduzzi P, Wu S, Sherstyukov B, Takahashi K. Changes in impacts of climate extremes: human systems and ecosystems. InManaging the risks of extreme events and disasters to advance climate change adaptation special report of the intergovernmental panel on climate change. Intergovernmental Panel on Climate Change, 2012: 231-290.
[15] McComas K, Shanahan J. Telling stories about global climate change: Measuring the impact of narratives on issue cycles. Communication research, 1999, 26(1): 30-57.
[16] Posner EA, Weisbach D. Climate change justice. Princeton University Press, 2010.
[17] Sodhi NS, Posa MR, Lee TM, Bickford D, Koh LP, Brook BW. The state and conservation of Southeast Asian biodiversity. Biodiversity and Conservation, 2010, 19(2): 317-28.
[18] Pyšek P, Richardson DM. Invasive species, environmental change and management, and health. Annual review of environment and resources, 2010, 35.
[19] Sodhi NS, Brook BW, Bradshaw CJ. Causes and consequences of species extinctions. The Princeton guide to ecology, 2009, 1(1): 514-20.
[20] WWF Pakistan. Climate Change in the Northern Areas Pakistan: Impacts on glaciers, ecology and livelihoods. Pakistan, 2008.
[21] National Academy of Sciences (NAS) 2001. Climate Change Science: An Analysis of Some Key Questions. National Academies Press. 2001: 42.
[22] Change, A.D.G. Climate change science: An analysis of some key questions. National Academies Press, 2001.
[23] Whitfield, S.M., et al. Amphibian and reptile declines over 35 years at La Selva, Costa Rica. Proceedings of the National Academy of Sciences, 2007. 104(20): 8352-8356.
[24] Cusack C. Fish, Justice, and Society. Brill, 2018.
[25] Leadley P. Biodiversity scenarios: projections of 21st century change in biodiversity, and associated ecosystem services: a technical report for the global biodiversity outlook 3. UNEP/Earthprint, 2010.
[26] Goeppert A, Czaun M, Prakash GS, Olah GA. Air as the renewable carbon source of the future: an overview of CO 2 capture from the atmosphere. Energy & Environmental Science. 2012, 5(7): 7833-53.
[27] Potts SG, Biesmeijer JC, Kremen C, Neumann P, Schweiger O, Kunin WE. Global pollinator declines: trends, impacts and drivers. Trends in ecology & evolution. 2010, 25(6): 345-53.

 DOI: https://doi.org/10.30564/jasr.v3i4.2275

BILINGUAL
PUBLISHING CO.
Pioneer of Global Academics Since 1984

Tel:+65 65881289
E-mail:contact@bilpublishing.com
Website:www.bilpublishing.com